Différentes modélisations a priori dans une approche bayésienne pour les problèmes inverses en imagerie

Ali MOHAMMAD-DJAFARI
Laboratoire des signaux et systèmes
Supélec, Plateau de Moulon
91192 Gif-sur-Yvette Cedex, FRANCE.

djafari@lss.supelec.fr
http://djafari.free.fr
http://www.lss.supelec.fr/perso/djafari

Plan de l'exposé

- Problèmes inverse en imagerie
- Méthodes algébriques déterministes
- Méthodes probabilistes
- Approche bayésienne
- Modélisations a priori
- Modèles séparables
- Modèles markoviens simples
- Modèles markoviens avec variables cachées lignes, contours et régions
- Aspects mise en oeuvres et calcul bayésien
- Exemples: Tomographie X, Imagerie microondes, Fusion d'images, Super-résolution, Séparation de sources, Imagerie hyperspectrale
- Conclusions

Problèmes inverses en imagerie: Tomographie

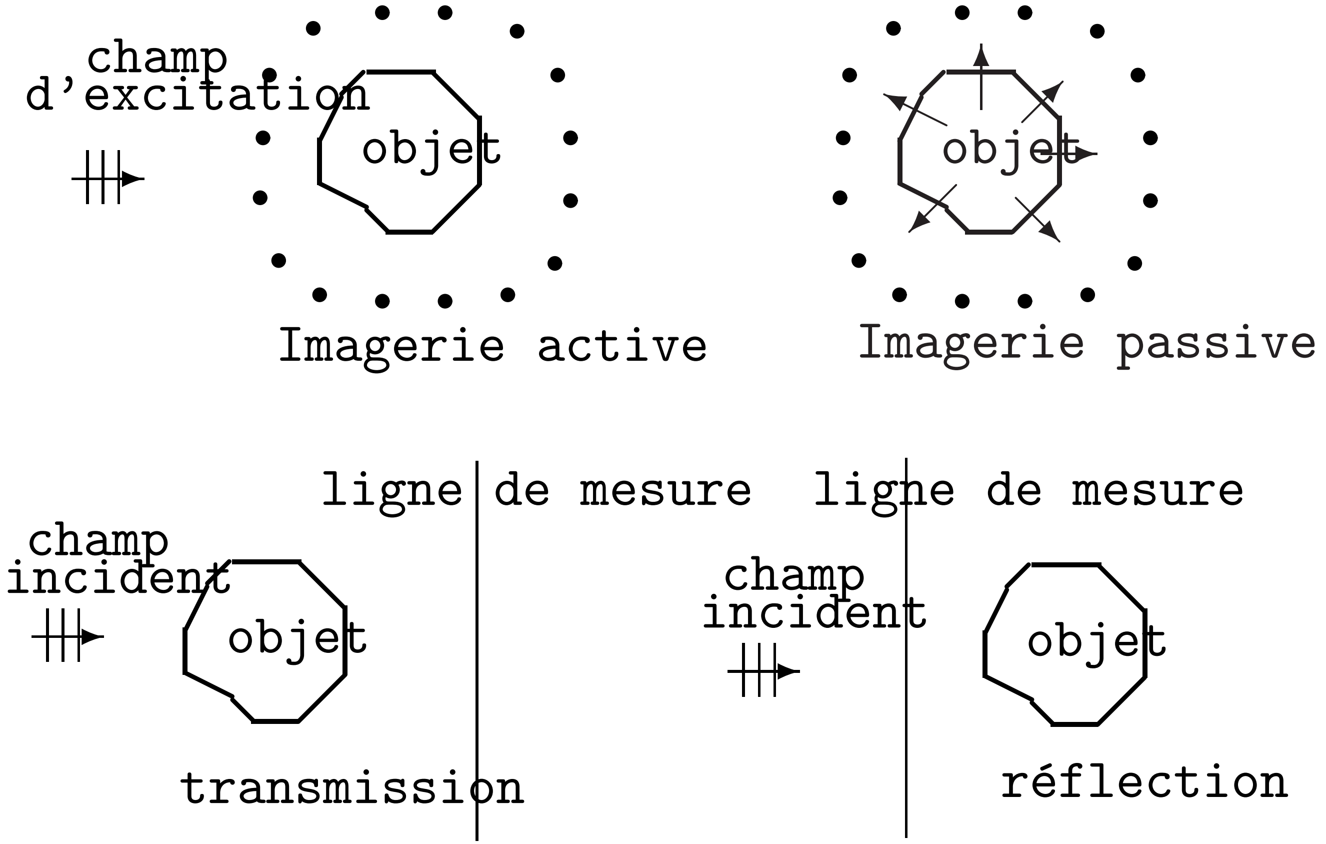

Problème directe: Connaisant l'objet calculer les mesures

Problème inverse: Connaisant les mesures trouver l'objet

Tomographie X

3D

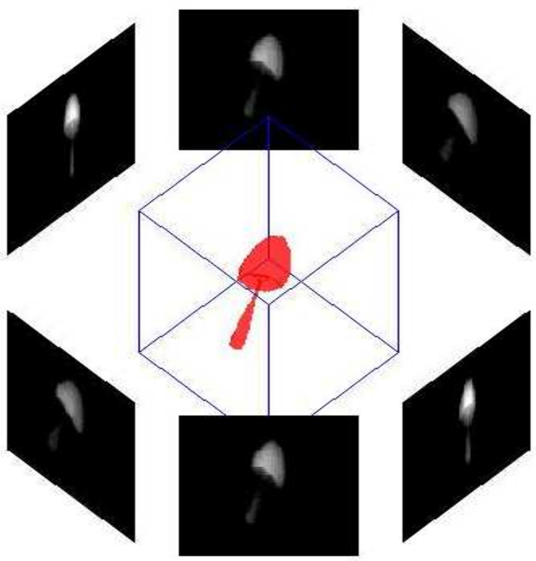

2D

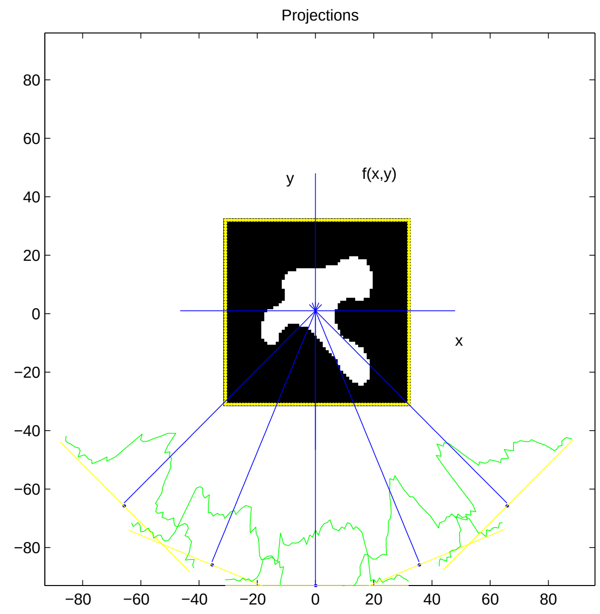

$$g_\phi(r_1,r_2) = \int_{\mathcal{L}_{r_1,r_2,\phi}} f(x,y,z) \,\mathrm{d}l \qquad g_\phi(r) = \int_{\mathcal{L}_{r,\phi}} f(x,y) \,\mathrm{d}l$$

- Problème directe: $f(x,y)$ ou $f(x,y,z) \longrightarrow g_\phi(r)$ or $g_\phi(r_1,r_2)$
- Problème inverse: $g_\phi(r)$ ou $g_\phi(r_1,r_2) \longrightarrow f(x,y)$ or $f(x,y,z)$

Tomographie X et Transformée de Radon

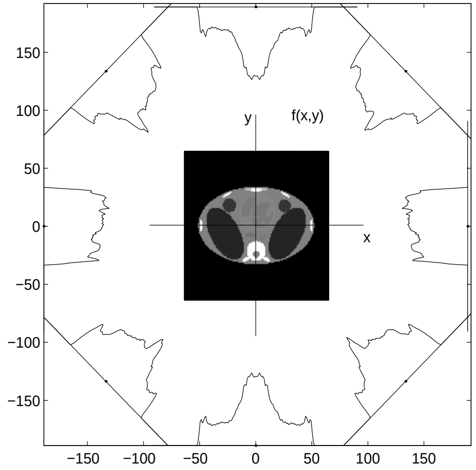

$$f(x,y) \longrightarrow \boxed{\text{TR}} \longrightarrow g(r,\phi)$$

$$g(r,\phi) = \int_{L_{r,\phi}} f(x,y) \; \mathrm{d}l$$

$$g(r,\phi) = \iint_D f(x,y)\, \delta(r - x\cos\phi - y\sin\phi) \; \mathrm{d}x \; \mathrm{d}y$$

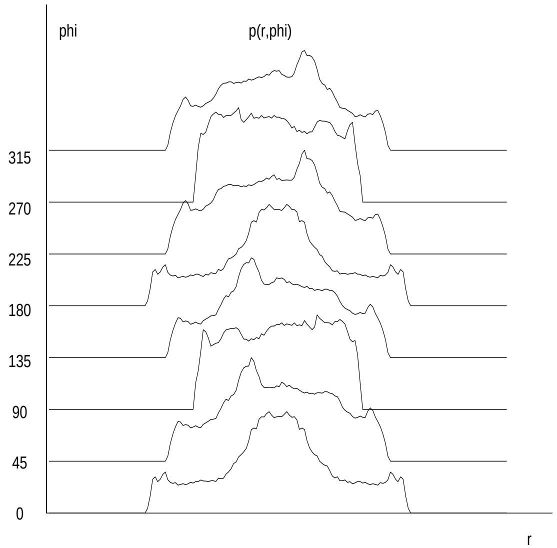

$$\overset{?}{\Longrightarrow}$$

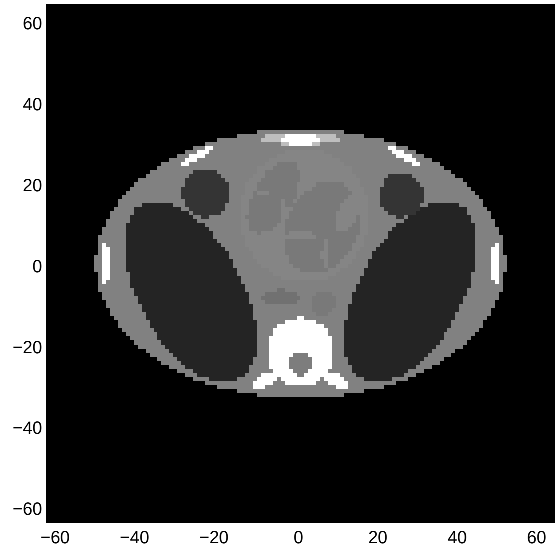

Tomographie X et Transformée de Radon

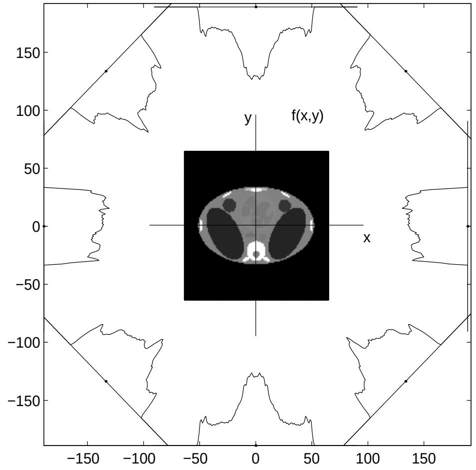

$$f(x,y) \longrightarrow \boxed{\text{TR}} \longrightarrow g(r,\phi)$$

$$g(r,\phi) = \int_{L_{r,\phi}} f(x,y) \; \mathrm{d}l$$

$$g(r,\phi) = \iint_D f(x,y)\, \delta(r - x\cos\phi - y\sin\phi) \; \mathrm{d}x \; \mathrm{d}y$$

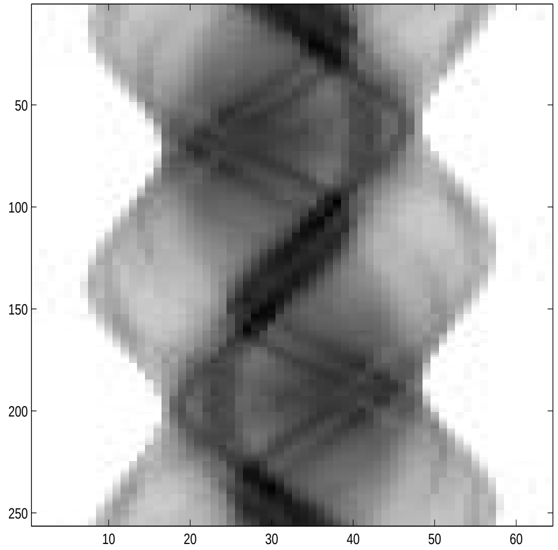

?

$\Longrightarrow$

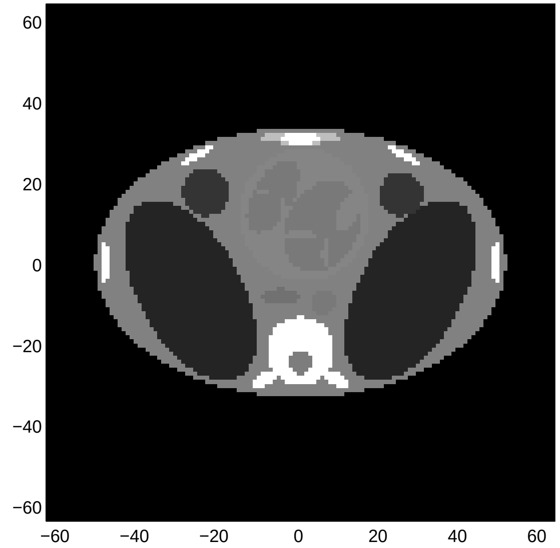

Méthodes d'inversion analytique

$$f(x,y) = \left(-\frac{1}{2\pi^2}\right) \int_0^\pi \int_{-\infty}^{+\infty} \frac{\frac{\partial}{\partial r} g(r,\phi)}{(r - x\cos\phi - y\sin\phi)} \, \mathrm{d}r \, \mathrm{d}\phi$$

Dérivation $\mathcal{D}$: $$\bar{g}(r,\phi) = \frac{\partial g(r,\phi)}{\partial r}$$

Transformée de Hilbert $\mathcal{H}$: $$g_1(r',\phi) = \frac{1}{\pi} \int_0^\infty \frac{\bar{g}(r,\phi)}{(r - r')} \, \mathrm{d}r$$

Rétroprojection $\mathcal{B}$: $$f(x,y) = \frac{1}{2\pi} \int_0^\pi g_1(r' = x\cos\phi + y\sin\phi, \phi) \, \mathrm{d}\phi$$

$$f(x,y) = \mathcal{B}\,\mathcal{H}\,\mathcal{D}\, g(r,\phi) = \mathcal{B}\, \mathcal{F}_1^{-1} \, |\Omega| \, \mathcal{F}_1 \, g(r,\phi)$$

- Rétroprojection des projections filtrées:

$$\xrightarrow{g(r,\phi)} \boxed{\begin{array}{c}\text{TF}\\ \mathcal{F}_1\end{array}} \longrightarrow \boxed{\begin{array}{c}\text{Filtre}\\ |\Omega|\end{array}} \longrightarrow \boxed{\begin{array}{c}\text{TFI}\\ \mathcal{F}_1^{-1}\end{array}} \xrightarrow{g_1(r,\phi)} \boxed{\begin{array}{c}\text{Rétroprojection}\\ \mathcal{B}\end{array}} \xrightarrow{f(x,y)}$$

Méthodes d'inversion algébrique

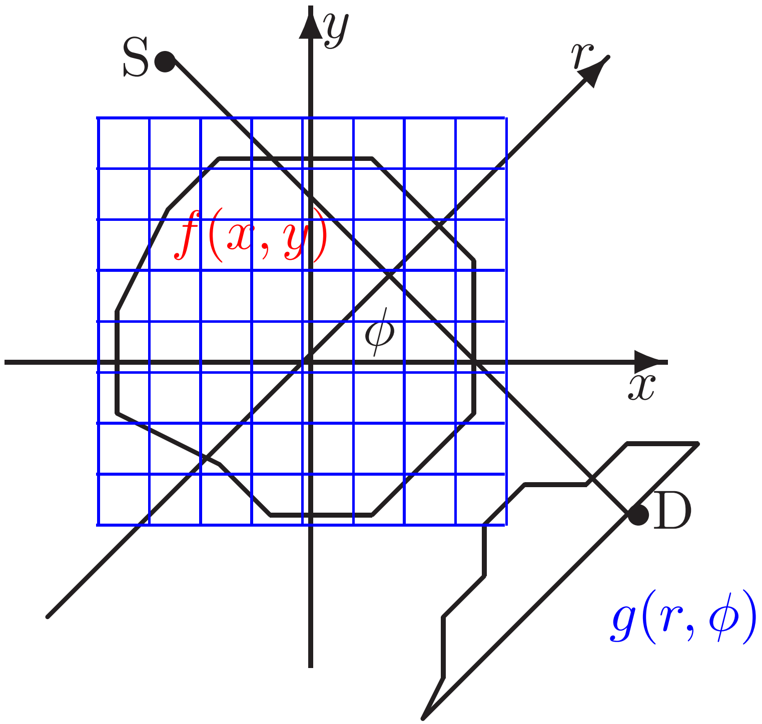

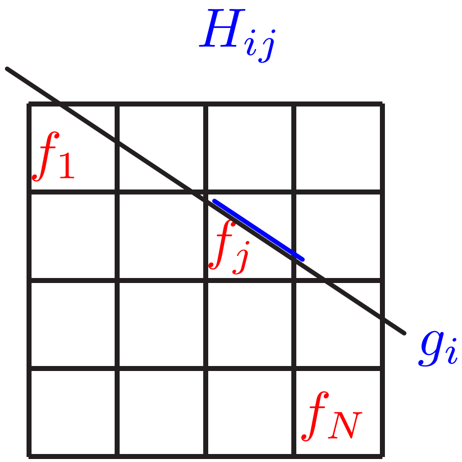

$$g(r,\phi) = \int_L f(x,y)\, \mathrm{d}l \qquad g_i = \sum_{j=1}^{N} H_{i,j}\, f_j$$

$$\boldsymbol{g} = \boldsymbol{H}\boldsymbol{f}$$

Méthodes d'inversion déterministe

Ingrédients de base :

- Un modèle directe : $\boldsymbol{g} = \boldsymbol{H}(\boldsymbol{f}) + \boldsymbol{\epsilon}$
- Une mesure d'adéquation aux données : $Q(\boldsymbol{g}, \boldsymbol{H}(\boldsymbol{f}))$
- Une paramétrisation $\boldsymbol{f}(\boldsymbol{\theta})$ ou une fonctionnelle de régularisation $\Phi(\boldsymbol{f})$

Méthodes d'inversion standard :

- Estimation paramétrique : $\widehat{\boldsymbol{\theta}} = \arg\min_{\boldsymbol{\theta}} \left\{Q(\boldsymbol{g}, \boldsymbol{H}(\boldsymbol{f}(\boldsymbol{\theta}))) = \|\boldsymbol{g} - \boldsymbol{H}(\boldsymbol{f}(\boldsymbol{\theta}))\|^2\right\}$
- Optimisation sous contraintes :

$$\widehat{\boldsymbol{f}} = \arg\min_{\boldsymbol{f}} \{\Phi(\boldsymbol{f})\} \quad \text{sous contrainte } \boldsymbol{g} = \boldsymbol{H}(\boldsymbol{f}) \quad \text{ou} \quad Q(\boldsymbol{g}, \boldsymbol{H}(\boldsymbol{f})) < \epsilon$$

- Critère régularisé :

$$\widehat{\boldsymbol{f}} = \arg\min_{\boldsymbol{f}} \{Q(\boldsymbol{g}, \boldsymbol{H}(\boldsymbol{f})) + \lambda\Phi(\boldsymbol{f})\}$$

Reconstruction d'image à partir de deux projections

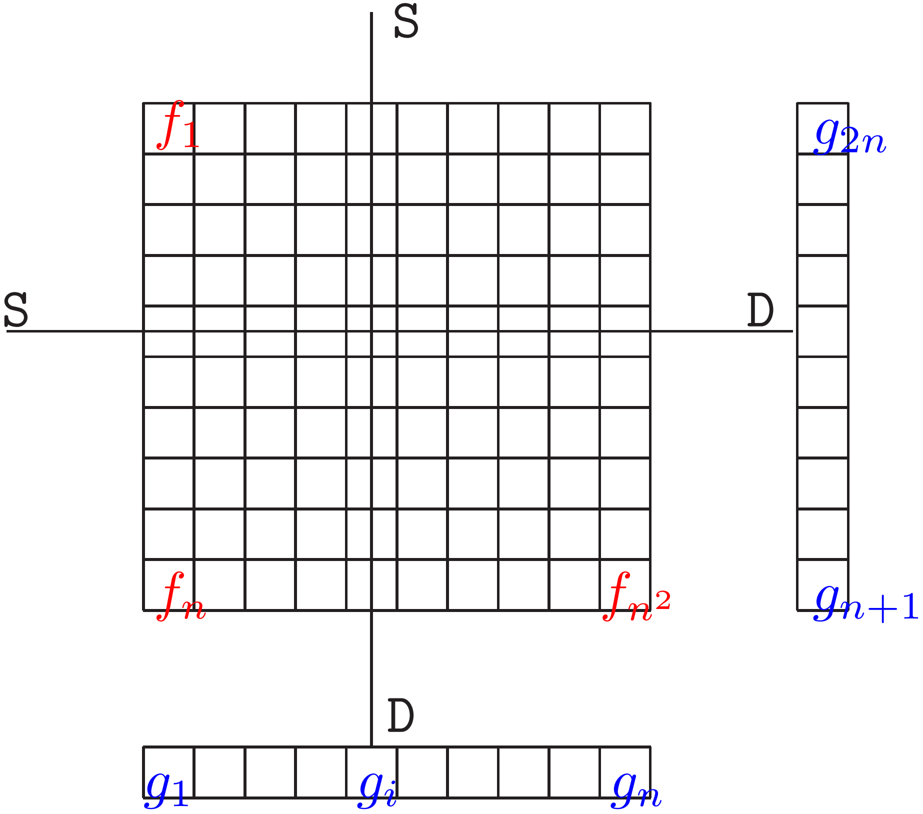

$\boldsymbol{g}_1 = \{g_1, \cdots, g_n\}$ horizontal

$\boldsymbol{g}_2 = \{g_{n+1}, \cdots, g_{2n}\}$ vertical

$$g_i = \sum_{j=1}^{N=n^2} H_{ij}\, f_j, \quad i = 1, \cdots M = 2n$$

$$H_{ij} = \{0, 1\}$$

$$\boldsymbol{f} = \{f_1, \cdots, f_N\}$$

$$\boldsymbol{g}_1 = \boldsymbol{H}_1 \boldsymbol{f}, \quad \boldsymbol{g}_2 = \boldsymbol{H}_2 \boldsymbol{f}$$

$$\boldsymbol{g} = \begin{bmatrix} \boldsymbol{g}_1 \\ \boldsymbol{g}_2 \end{bmatrix}, \quad \boldsymbol{H} = \begin{bmatrix} \boldsymbol{H}_1 \\ \boldsymbol{H}_2 \end{bmatrix}$$

$$\boldsymbol{g} = \boldsymbol{H} \boldsymbol{f}$$

Limites des méthodes analytiques et déterministes

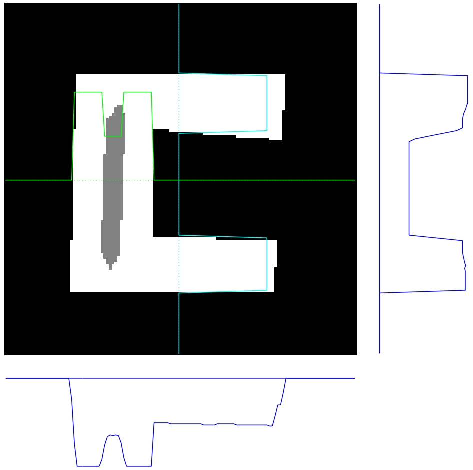

Original

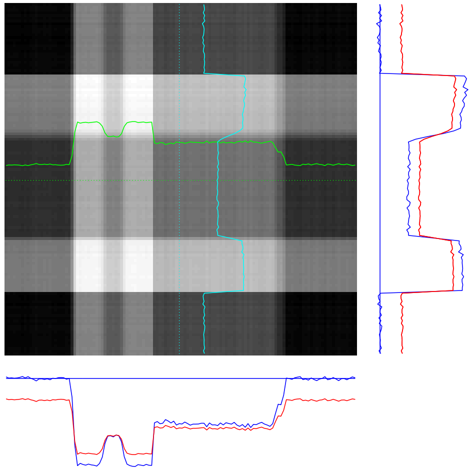

Rétroprojection

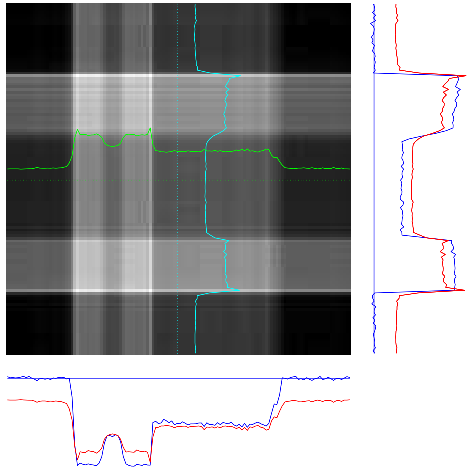

Rétroprojection Filtée

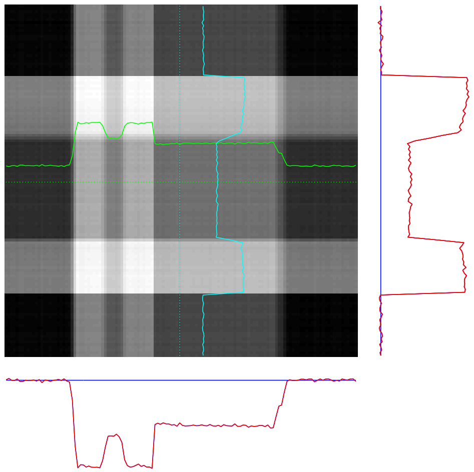

MC

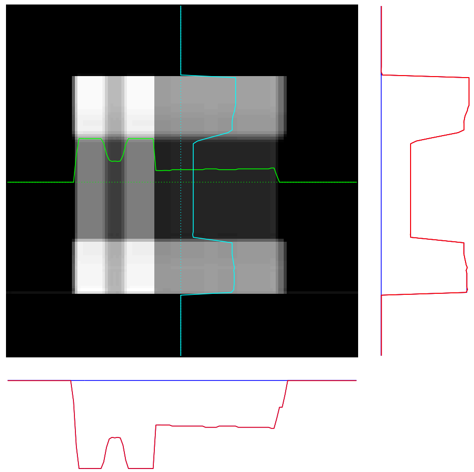

Rég. + positivité + support

Méthodes probabilistes

Maximum de vraisemblance (MV)

$$\left\{\begin{array}{ll}\text{Modèle d'observation :} & \boldsymbol{g} = \boldsymbol{H}(\boldsymbol{f}) + \boldsymbol{\epsilon} \\ \text{Caractéristiques du bruit :} & p_\epsilon(\boldsymbol{\epsilon})\end{array}\right. \longrightarrow p(\boldsymbol{g}|\boldsymbol{f})$$

$$\widehat{\boldsymbol{f}} = \arg\max_{\boldsymbol{f}} \{p(\boldsymbol{g}|\boldsymbol{f})\} = \arg\min_{\boldsymbol{f}} \{-\ln p(\boldsymbol{g}|\boldsymbol{f})\}$$

- Cas linéaire gaussien : $\longrightarrow$ Moindres Carrés
- Méthode rarement satisfaisante pour les problèmes inverses
- Maximum de vraisemblance pénalisée

$$\widehat{\boldsymbol{f}} = \arg\min_{\boldsymbol{f}} \{-\ln p(\boldsymbol{g}|\boldsymbol{f}) + \Phi(\boldsymbol{f})\}$$

Approche estimation bayésienne

Ingrédients de base :

- Modèle directe : $\boldsymbol{g} = \boldsymbol{H}(\boldsymbol{f}) + \boldsymbol{\epsilon}$
- Mesure d'adéquation aux données : $p(\boldsymbol{g}|\boldsymbol{f}) = p_{\boldsymbol{\epsilon}}(\boldsymbol{g} - \boldsymbol{H}(\boldsymbol{f}))$
- Information *a priori* $p(\boldsymbol{f})$
- Règle de Bayes : $p(\boldsymbol{f}|\boldsymbol{g}) = \dfrac{p(\boldsymbol{g}|\boldsymbol{f})\, p(\boldsymbol{f})}{p(\boldsymbol{g})} \propto p(\boldsymbol{g}|\boldsymbol{f})\, p(\boldsymbol{f})$
- Choix d'un estimateur $\widehat{\boldsymbol{f}} = \arg\min_{\boldsymbol{f}'} \left\{ \int C(\boldsymbol{f}' - \boldsymbol{f}) p(\boldsymbol{f}|\boldsymbol{g}) \,\mathrm{d}\boldsymbol{f} \right\}$

Lien avec régularisation :

- Estimation au sens du maximum *a posteriori* (MAP) :

$$\widehat{\boldsymbol{f}} = \arg\max_{\boldsymbol{f}} \{\ln p(\boldsymbol{f}|\boldsymbol{g}) = \ln p(\boldsymbol{g}|\boldsymbol{f}) + \ln p(\boldsymbol{f})\}$$

$$\text{avec} \quad Q(\boldsymbol{g}, \boldsymbol{H}(\boldsymbol{f})) = \ln p(\boldsymbol{g}|\boldsymbol{f}) \quad \text{et} \quad \Phi(\boldsymbol{f}) = \ln p(\boldsymbol{f})$$

Cas linéaire et modèles a priori Gaussiens

$$\boldsymbol{g} = \boldsymbol{H}\boldsymbol{f} + \boldsymbol{\epsilon}$$

- Hypothèse sur les erreurs: $\boldsymbol{\epsilon} \sim \mathcal{N}(\mathbf{0}, \sigma_\epsilon^2 \boldsymbol{I})$
  $\longrightarrow \boldsymbol{g}|\boldsymbol{f} \sim \mathcal{N}(\boldsymbol{H}\boldsymbol{f}, \beta\boldsymbol{I}) \longrightarrow p(\boldsymbol{g}|\boldsymbol{f}) \propto \exp\left[-\beta\|\boldsymbol{g}-\boldsymbol{H}\boldsymbol{f}\|^2\right], \quad \beta = \frac{1}{2\sigma_\epsilon^2}$
- Modèle a priori $\boldsymbol{f}$:
  $$\boldsymbol{f} \sim \mathcal{N}(\mathbf{0}, \sigma_f^2(\boldsymbol{D}^t\boldsymbol{D})^{-1}) \longrightarrow p(\boldsymbol{f}) \propto \exp\left[-\alpha\|\boldsymbol{D}\boldsymbol{f}\|^2\right], \quad \alpha = \frac{1}{2\sigma_f^2}$$
- A posteriori:
  $$p(\boldsymbol{f}|\boldsymbol{g}) \propto \exp\left[-\|\boldsymbol{g}-\boldsymbol{H}\boldsymbol{f}\|^2 + \lambda\|\boldsymbol{D}\boldsymbol{f}\|^2\right] \qquad \lambda = \frac{\sigma_\epsilon^2}{\sigma_f^2} = \frac{\alpha}{\beta}$$
- MAP : $\quad \widehat{\boldsymbol{f}} = \arg\max_{\boldsymbol{f}} \{p(\boldsymbol{f}|\boldsymbol{g})\} = \arg\min_{\boldsymbol{f}} \{J(\boldsymbol{f})\}$
  $$\text{avec} \qquad J(\boldsymbol{f}) = \|\boldsymbol{g}-\boldsymbol{H}\boldsymbol{f}\|^2 + \lambda\|\boldsymbol{D}\boldsymbol{f}\|^2$$
- Avantage : caractérisation de la solution
  $$\boldsymbol{f}|\boldsymbol{g} \sim \mathcal{N}(\widehat{\boldsymbol{f}}, \widehat{\boldsymbol{P}}) \;\text{ avec }\; \widehat{\boldsymbol{f}} = \widehat{\boldsymbol{P}}\boldsymbol{H}^t\boldsymbol{g}, \quad \widehat{\boldsymbol{P}} = \left(\boldsymbol{H}^t\boldsymbol{H} + \lambda\boldsymbol{D}^t\boldsymbol{D}\right)^{-1}$$

Modèles gaussiens en terme de variables cachées

$$\left\{\begin{array}{l} \boldsymbol{g}=\boldsymbol{H}\boldsymbol{f}+\boldsymbol{\epsilon} \\ \text{avec } \ \boldsymbol{f}\sim\mathcal{N}\left(\mathbf{0},\sigma_f^2(\boldsymbol{D}^t\boldsymbol{D})^{-1})\right) \end{array}\right. = \left\{\begin{array}{l} \boldsymbol{g}=\boldsymbol{H}\boldsymbol{f}+\boldsymbol{\epsilon} \\ \boldsymbol{f}=\boldsymbol{C}\boldsymbol{f}+\boldsymbol{z} \ \text{ avec } \ \boldsymbol{z}\sim\mathcal{N}(\mathbf{0},\sigma_f^2\boldsymbol{I}) \\ \text{ et } \boldsymbol{D}=(\boldsymbol{I}-\boldsymbol{C}) \end{array}\right.$$

$$\boldsymbol{f}|\boldsymbol{g}\sim\mathcal{N}(\widehat{\boldsymbol{f}},\widehat{\boldsymbol{P}}) \ \text{ avec } \ \widehat{\boldsymbol{f}}=\widehat{\boldsymbol{P}}\boldsymbol{H}^t\boldsymbol{g}, \quad \widehat{\boldsymbol{P}}=\left(\boldsymbol{H}^t\boldsymbol{H}+\lambda\boldsymbol{D}^t\boldsymbol{D}\right)^{-1}$$

$$\left\{\begin{array}{l} \boldsymbol{g}=\boldsymbol{H}\boldsymbol{f}+\boldsymbol{\epsilon} \\ \text{avec } \ \boldsymbol{f}\sim\mathcal{N}\left(\mathbf{0},\sigma_f^2(\boldsymbol{D}\boldsymbol{D}^t)\right) \end{array}\right. = \left\{\begin{array}{l} \boldsymbol{g}=\boldsymbol{H}\boldsymbol{f}+\boldsymbol{\epsilon} \\ \boldsymbol{f}=\boldsymbol{D}\boldsymbol{z} \ \text{ avec } \ \boldsymbol{z}\sim\mathcal{N}(\mathbf{0},\sigma_f^2\boldsymbol{I}) \end{array}\right.$$

$$\boldsymbol{z}|\boldsymbol{g}\sim\mathcal{N}(\widehat{\boldsymbol{z}},\widehat{\boldsymbol{P}}) \ \text{ avec } \ \widehat{\boldsymbol{z}}=\widehat{\boldsymbol{P}}\boldsymbol{D}^t\boldsymbol{H}^t\boldsymbol{g}, \quad \widehat{\boldsymbol{P}}=\left(\boldsymbol{D}^t\boldsymbol{H}^t\boldsymbol{H}\boldsymbol{D}+\lambda\boldsymbol{I}\right)^{-1} \longrightarrow \widehat{\boldsymbol{f}}=\boldsymbol{D}\widehat{\boldsymbol{z}}$$

$\boldsymbol{z}$ coéfficients de décomposition sur une base (colonnes de $\boldsymbol{D}$ forment une base)

Modélisations a priori

- Modèles séparables $p(\boldsymbol{f}) = \prod_j p_j(f_j) \propto \exp\left[-\beta \sum_j \phi(f_j)\right]$ ou

$$p(\boldsymbol{f}) \propto \exp\left[-\beta \sum_{\boldsymbol{r}\in\mathcal{R}} \phi(f(\boldsymbol{r}))\right]$$

- Modèles markoviens simples $p(f_j|f_{j-1}) \propto \exp\left[-\beta\phi(f_j - f_{j-1})\right]$ ou

$$p(\boldsymbol{f}) \propto \exp\left[-\beta \sum_{\boldsymbol{r}\in\mathcal{R}} \sum_{\boldsymbol{r}'\in\mathcal{V}(\boldsymbol{r})} \phi(f(\boldsymbol{r}), f(\boldsymbol{r}'))\right]$$

- Modèles markoviens avec variables cachées $z(\boldsymbol{r})$ (lignes, contours, frontières et régions)

$$p(\boldsymbol{f}|\boldsymbol{z}) \propto \exp\left[-\beta \sum_{\boldsymbol{r}\in\mathcal{R}} \sum_{\boldsymbol{r}'\in\mathcal{V}(\boldsymbol{r})} \phi(f(\boldsymbol{r}), f(\boldsymbol{r}'), z(\boldsymbol{r}), z(\boldsymbol{r}'))\right]$$

Estimation au sens du MAP ou régularisation:

$$\widehat{\boldsymbol{f}} = \arg\min_{\boldsymbol{f}} \{J(\boldsymbol{f})\} \quad \text{avec} \quad J(\boldsymbol{f}) = \|\boldsymbol{g} - \boldsymbol{H}(\boldsymbol{f})\|^2 + \lambda\Phi(\boldsymbol{f})$$

- Lois gaussiennes: $\Phi(\boldsymbol{f})$ quadratique
  $\longrightarrow J(\boldsymbol{f})$ quadratique $\longrightarrow \widehat{\boldsymbol{f}}$ fonction linéaire de $\boldsymbol{g}$ $\longrightarrow$ Algorithmes rapides
- Lois non gaussiennes mais $\Phi(\boldsymbol{f})$ convexe:
  Exemples: $\Phi(\boldsymbol{f}) = \sum_j \phi(f_j)$ ou $\Phi(\boldsymbol{f}) = \sum_j \phi(f_j - f_{j-1})$
  avec $\phi(t) = \{|t|^p, \quad (|t| \ln |t| - |t|), \quad (\ln(1 + |t|)\}$
  $\longrightarrow J(\boldsymbol{f})$ convexe $\longrightarrow$ Estimation nonlinéair mais facile à calculer
- Lois non gaussiennes et $\Phi(\boldsymbol{f})$ non convexe:
  Exemples:
  $$\Phi(t) = \begin{cases} |t|^2 & \text{if } |t| < \alpha, \\ \alpha^2 & \text{else,} \end{cases}, \begin{cases} t^2 & \text{if } |t| < \alpha, \\ 2\alpha t - \alpha^2 & \text{else,} \end{cases}, \frac{\alpha^2 t^2}{1+t^2}, \quad \log\cosh(t/\alpha)$$
  $\longrightarrow J(\boldsymbol{f})$ non convexe $\longrightarrow$ Minima locaux $\longrightarrow$ Optimisation globale

Modèles séparables

- Gaussienne:

$$p(f_j) \propto \exp\left[-\alpha(f_j - m_j)^2\right] \longrightarrow \quad \Omega(\boldsymbol{f}) = \alpha \sum_j (f_j - m_j)^2$$

- Gamma:

$$p(f_j) \propto (f_j/m_j)^{\alpha} \exp\left[-f_j/m_j\right] \longrightarrow \quad \Omega(\boldsymbol{f}) = \alpha \sum_j \ln \frac{f_j}{m_j} + \frac{f_j}{m_j},$$

- Béta:

$$p(f_j) \propto f_j^{\alpha} (1 - f_j)^{\beta} \longrightarrow \quad \Omega(\boldsymbol{f}) = \alpha \sum_j \ln f_j + \beta \sum_j \ln(1 - f_j),$$

- Gaussienne généraliée:

$$p(f_j) \propto \exp\left[-\alpha |f_j - m_j|^p\right], \quad 1 < p < 2 \longrightarrow \quad \Phi(\boldsymbol{f}) = \alpha \sum_j |f_j - m_j|^p,$$

Modèles markoviens simples

$$p(f_j|\boldsymbol{f}) \propto \exp\left[-\alpha \sum_{i \in N_j} \phi(f_j, f_i)\right] \longrightarrow \quad \Phi(\boldsymbol{f}) = \alpha \sum_j \sum_{i \in V_j} \phi(f_j, f_i)$$

- Cas 1D et un seul voisin $V_j = j-1$:

$$\Phi(\boldsymbol{f}) = \alpha \sum_j \phi(f_j, f_{j-1}) = \alpha \sum_j \phi(f_j - f_{j-1})$$

- Cas 1D et deux voisins $V_j = \{j-1, j+1\}$:

$$\Phi(\boldsymbol{f}) = \alpha \sum_j \phi\left(f_j - (\beta_1 f_{j-1} + \beta_2 f_{j-1})\right) = \alpha \sum_j \phi\left(f_j - \boldsymbol{\beta}^t \boldsymbol{f}_{\mathcal{V}(j)}\right)$$

- Cas 2D et les quatres voisins:

$$\Phi(\boldsymbol{f}) = \alpha \sum_{\boldsymbol{r} \in \mathcal{R}} \sum_{\boldsymbol{r}' \in \mathcal{V}(\boldsymbol{r})} \phi(f(\boldsymbol{r}), f(\boldsymbol{r}')) = \alpha \sum_{\boldsymbol{r} \in \mathcal{R}} \phi\left(f(\boldsymbol{r}) - \beta \sum_{\boldsymbol{r}' \in \mathcal{V}(\boldsymbol{r})} f(\boldsymbol{r}')\right)$$

- $\phi(t) = |t|^\gamma$: Gaussienne généraliée

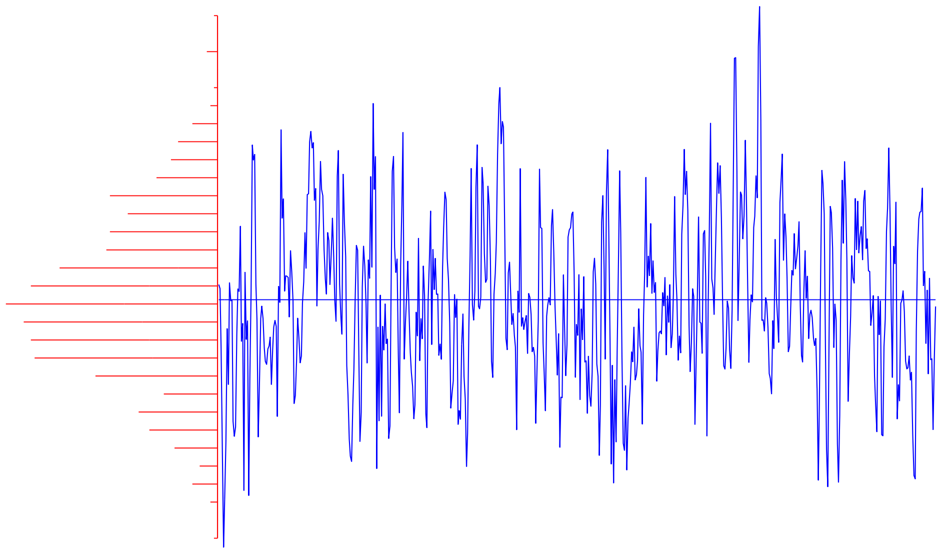

Gaussienne

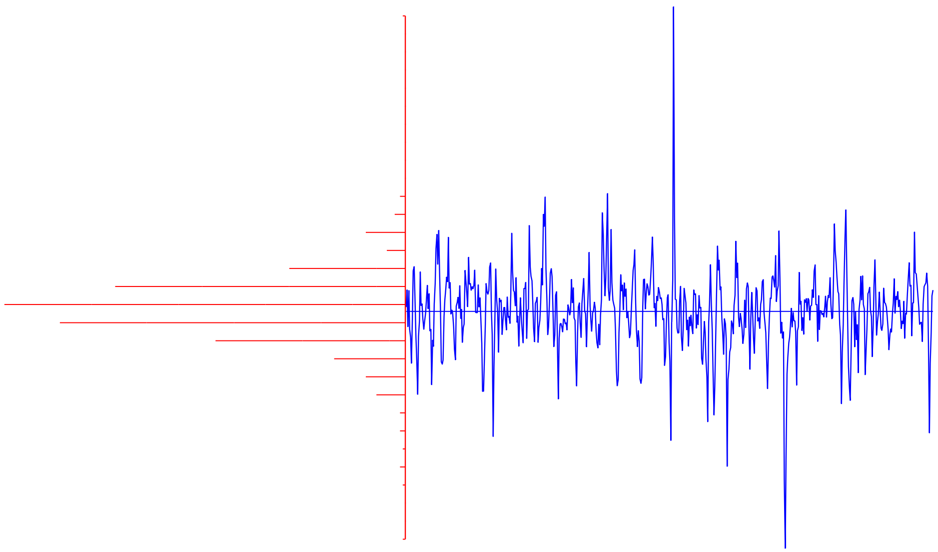

Gaussienne généralisée

$$p(f_j|f_{j-1}) = \mathcal{N}(f_{j-1}, \sigma_f^2)$$

$$p(\boldsymbol{f}) \propto \exp\left[-\alpha \sum_j |f_j - f_{j-1}|^2\right]$$

$$p(\boldsymbol{f}) \propto \exp\left[-\alpha \sum_{\boldsymbol{r}\in\mathcal{R}} |f(\boldsymbol{r}) - \beta \sum_{\boldsymbol{r}'\in\mathcal{V}(\boldsymbol{r})} f(\boldsymbol{r}')|^2\right]$$

$$p(f_j|f_{j-1}) \propto \exp\left[-\alpha|f_j - f_{j-1}|^p\right]$$

$$p(\boldsymbol{f}) \propto \exp\left[-\alpha \sum_j |f_j - f_{j-1}|^p\right]$$

$$p(\boldsymbol{f}) \propto \exp\left[-\alpha \sum_{\boldsymbol{r}\in\mathcal{R}} |f(\boldsymbol{r}) - \beta \sum_{\boldsymbol{r}'\in\mathcal{V}(\boldsymbol{r})} f(\boldsymbol{r}')|^p\right]$$

Modèles markoviens avec des variables cachées

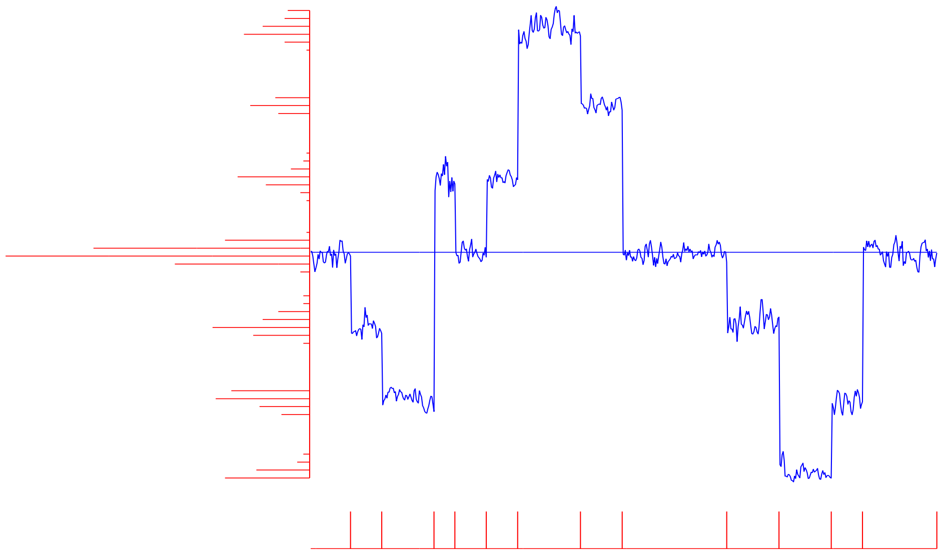

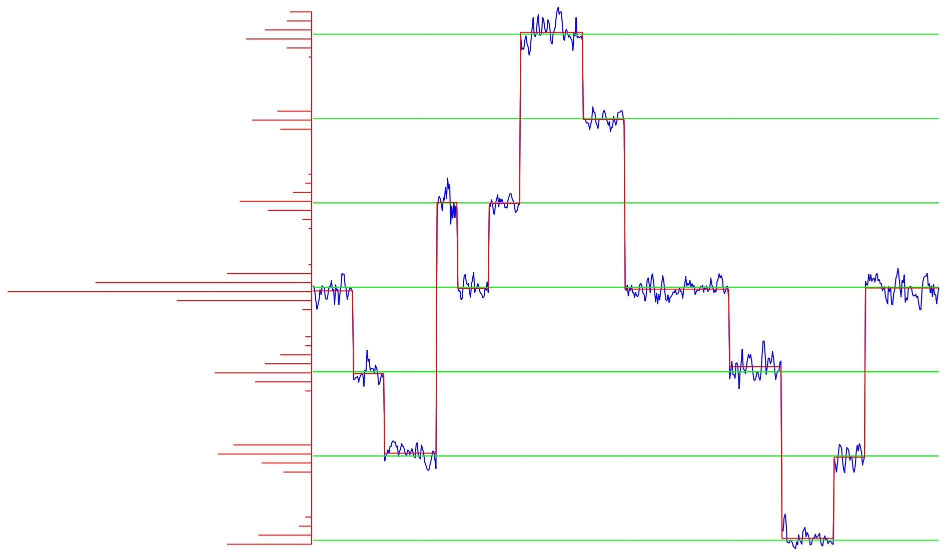

Gaussiennes par morceaux | Mélange de gaussiennes

(variables cachées ligne ou contours) | (variables cachées étiquettes des régions)

$$p(f_j|q_j, f_{j-1}) = \mathcal{N}\left((1-q_j)f_{j-1}, \sigma_f^2\right) \qquad p(f_j|z_j = k, f_{j-1}) = \mathcal{N}\left(m_k, \sigma_k^2\right)$$

$$p(\boldsymbol{f}|\boldsymbol{q}) \propto \exp\left[-\alpha \sum_j (1-q_j)|f_j - f_{j-1}|^2\right] \qquad p(\boldsymbol{f}|\boldsymbol{z}) \propto \exp\left[-\alpha \sum_k \sum_{j\in\mathcal{R}_k} \left(\frac{f_j - m_k}{\sigma_k}\right)^2\right]$$

Modèles markoviens avec des variables cachées

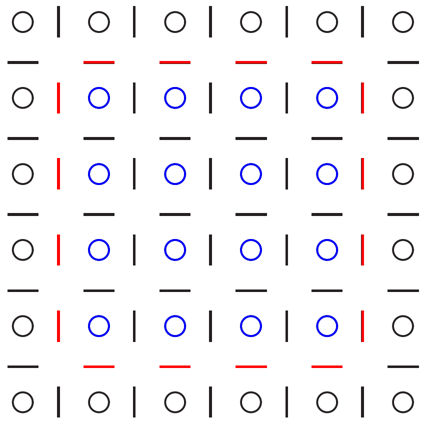

$f(\boldsymbol{r})$ intensités

$l(\boldsymbol{r},\boldsymbol{r}')$ lignes

$q(\boldsymbol{r},\boldsymbol{r}')$ contours

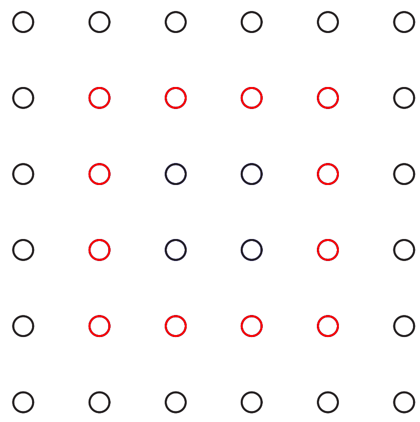

$f(\boldsymbol{r})$ intensités

$z(\boldsymbol{r})$ étiquettes régions

$q(\boldsymbol{r})$ frontières des régions

$\mathcal{R} = \{(i,j) : 1 \leq i \leq m, 1 \leq j \leq n\}$ sites pixels $\circ$ sites lignes $-$

$\mathcal{R}_k = \{\boldsymbol{r} : \boldsymbol{r} \in \mathcal{R}_k\}, \quad \cup_k \mathcal{R}_k = \mathcal{R}$ régions

$\boldsymbol{f} = \{f(\boldsymbol{r}), \boldsymbol{r} \in \mathcal{R}\}$ image (intensités)

$\boldsymbol{l} = \{l(\boldsymbol{r}), \boldsymbol{r} \in \mathcal{R}\}$ (ou $l(\boldsymbol{r},\boldsymbol{r}')$) lignes $l(\boldsymbol{r}) \in [0,1]$

$\boldsymbol{q} = \{q(\boldsymbol{r}), \boldsymbol{r} \in \mathcal{R}\}$ (ou $q(\boldsymbol{r},\boldsymbol{r}')$) contours $q(\boldsymbol{r}) \in \{0,1\}$

$\boldsymbol{z} = \{z(\boldsymbol{r}), \boldsymbol{r} \in \mathcal{R}\}$ étiquette région $z(\boldsymbol{r}) \in \{0, \cdots, K\}$

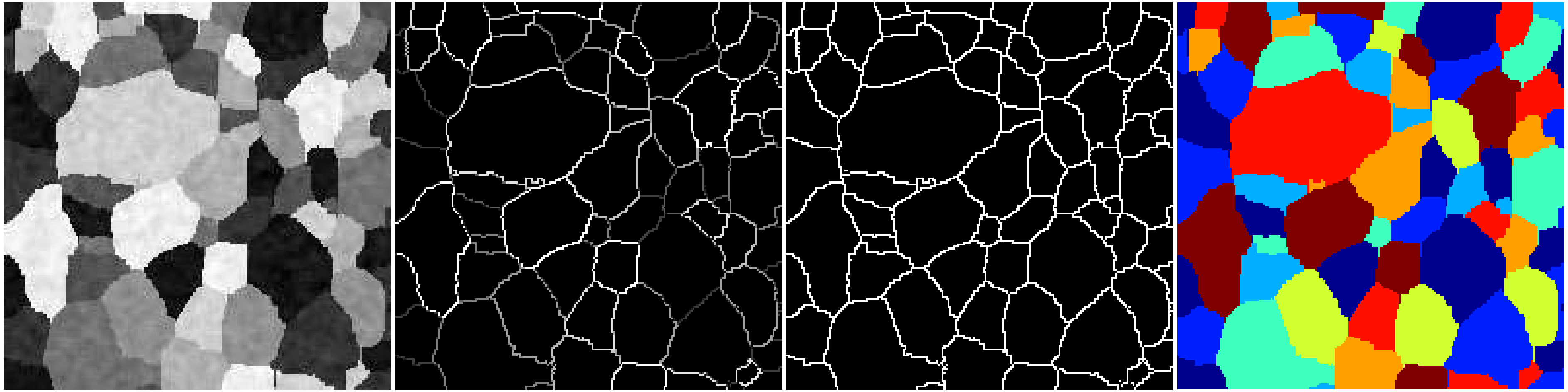

$f(\boldsymbol{r})$ $\quad$ $l(\boldsymbol{r}) \in [0,1]$ $\quad$ $q(\boldsymbol{r}) \in \{0,1\}$ $\quad$ $z(\boldsymbol{r}) \in \{1,\cdots,K\}$

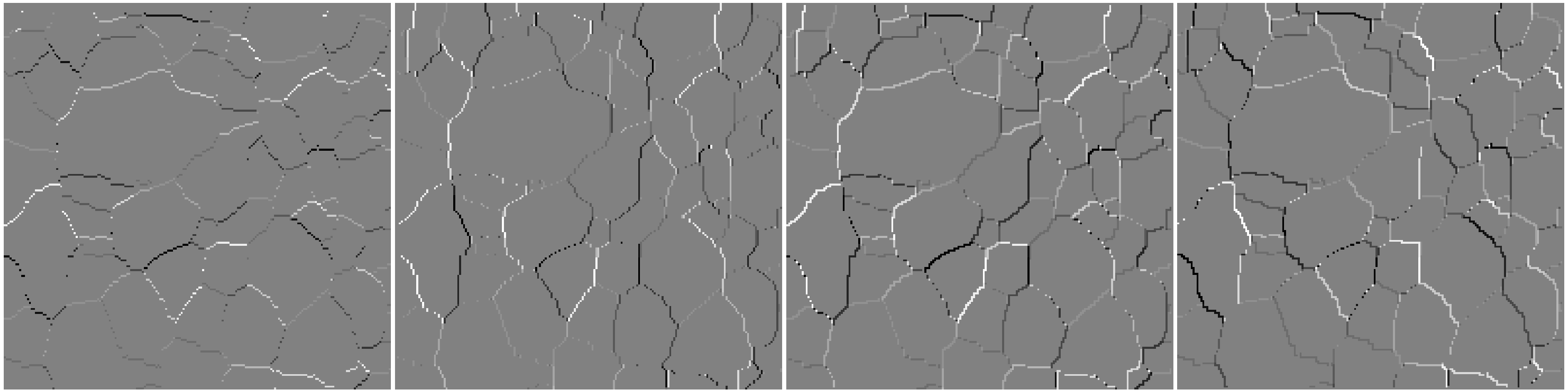

$l_h(\boldsymbol{r})$ $\quad$ $l_v(\boldsymbol{r})$ $\quad$ $l_{hv}(\boldsymbol{r})$ $\quad$ $l_{vh}(\boldsymbol{r})$

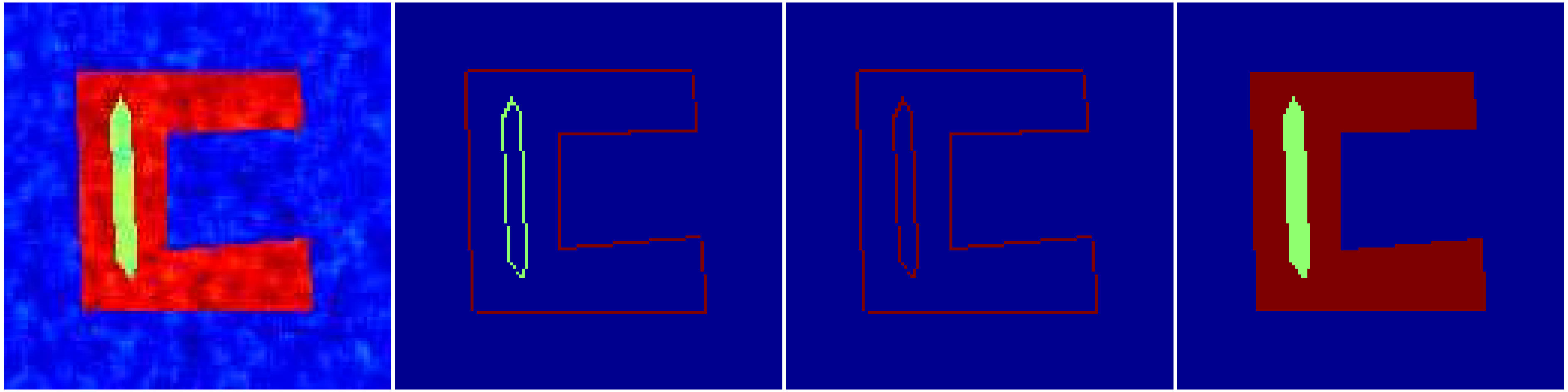

$f(\boldsymbol{r})$ $l(\boldsymbol{r})$ $q(\boldsymbol{r})$ $z(\boldsymbol{r})$

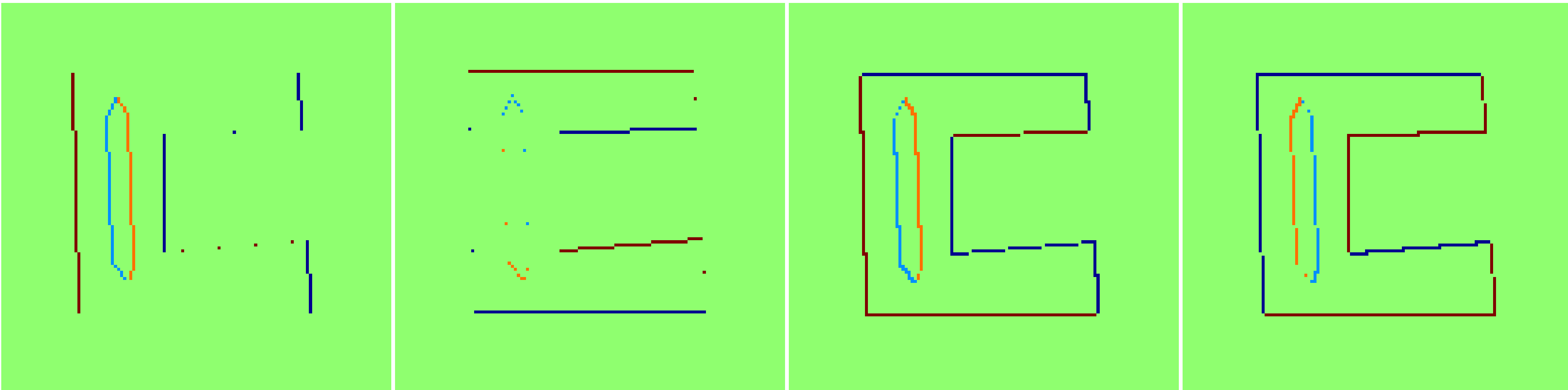

$l_x(\boldsymbol{r})$ $l_y(\boldsymbol{r})$ $l_{yx}(\boldsymbol{r})$ $l_{xy}(\boldsymbol{r})$

Modèles de Gauss-Markov (signaux et images continus)

$\boldsymbol{g} = \boldsymbol{H} \boldsymbol{f} + \boldsymbol{\epsilon}$

$f(\boldsymbol{r})$ image continue : Gauss-Markov

$$p(f(\boldsymbol{r})|f(\boldsymbol{r}')) = \mathcal{N}\left(\beta \sum_{\boldsymbol{r}' \in \mathcal{V}(\boldsymbol{r})} f(\boldsymbol{r}'), \sigma_f^2\right)$$

MAP :

$$\widehat{\boldsymbol{f}} = \arg\max_{\boldsymbol{f}} \{p(\boldsymbol{f}|\boldsymbol{g})\} = \arg\min_{\boldsymbol{f}} \{J(\boldsymbol{f})\}$$

$$J(\boldsymbol{f}) = \|\boldsymbol{g} - \boldsymbol{H}\boldsymbol{f}\|^2 + \sum_{\boldsymbol{r}} \left(f(\boldsymbol{r}) - \beta \sum_{\boldsymbol{r}' \in \mathcal{V}(\boldsymbol{r})} f(\boldsymbol{r}')\right)^2$$

MAP =Régularisation quadratique

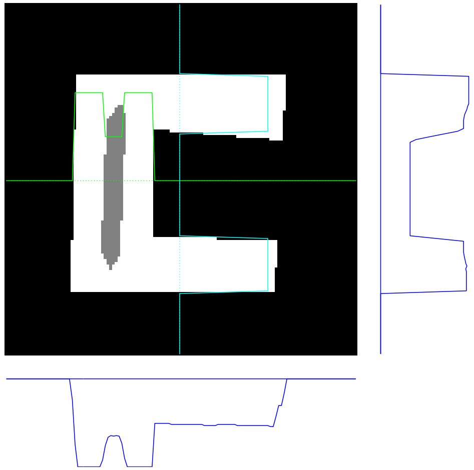

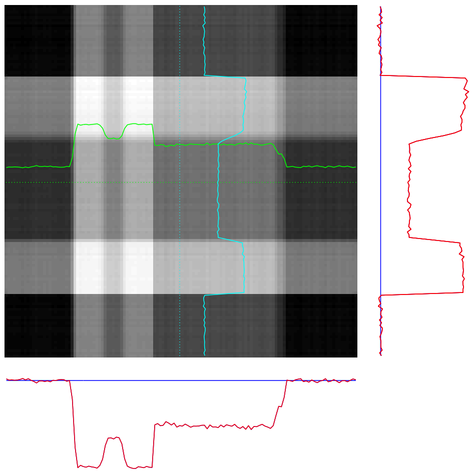

Modèles markoviens avec variables cachées lignes

$\boldsymbol{g} = \boldsymbol{H}\boldsymbol{f} + \boldsymbol{\epsilon}$,

$f(\boldsymbol{r})$ images continues par morceaux :

Variables cachée lignes ou contours: $q(\boldsymbol{r})$

$$p(f(\boldsymbol{r})|q(\boldsymbol{r}), f(\boldsymbol{r}')) = \mathcal{N}\left(\beta(1-q(\boldsymbol{r}))\sum_{\boldsymbol{r}'\in\mathcal{V}(\boldsymbol{r})} f(\boldsymbol{r}'), \sigma_f^2\right)$$

$$\text{MAP : } (\widehat{\boldsymbol{f}}, \widehat{\boldsymbol{q}}) = \arg\max_{\boldsymbol{f},\boldsymbol{q}} \{p(\boldsymbol{f}, \boldsymbol{q}|\boldsymbol{g})\}$$

$$\widehat{\boldsymbol{f}} = \arg\max_{\boldsymbol{f}} \{p(\boldsymbol{f}|\boldsymbol{g}, \boldsymbol{q})\} = \arg\min_{\boldsymbol{f}} \{J(\boldsymbol{f})\}$$

$$J(\boldsymbol{f}) = \|\boldsymbol{g} - \boldsymbol{H}\boldsymbol{f}\|^2 + \sum_{\boldsymbol{r}}(1-q(\boldsymbol{r}))\left(f(\boldsymbol{r}) - \beta\sum_{\boldsymbol{r}'\in\mathcal{V}(\boldsymbol{r})} f(\boldsymbol{r}')\right)^2$$

$$\widehat{\boldsymbol{q}} = \arg\max_{\boldsymbol{q}} \{p(\boldsymbol{q}|\boldsymbol{g})\}$$

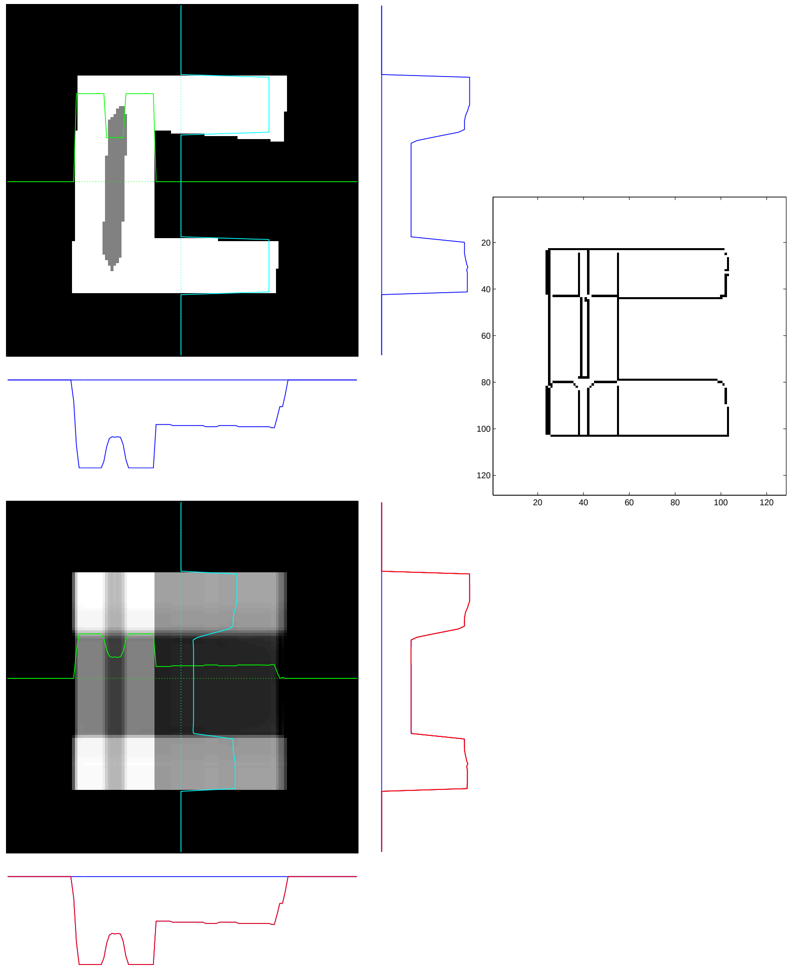

Modèles markoviens avec variables cachées lignes

Lien entre modles variables caches et potentiels non convexes

$$(\widehat{\boldsymbol{f}}, \widehat{\boldsymbol{q}}) = \arg\max_{\boldsymbol{f},\boldsymbol{q}} \{p(\boldsymbol{f}, \boldsymbol{q}|\boldsymbol{g})\}$$

$$\widehat{\boldsymbol{f}} = \arg\max_{\boldsymbol{f}} \{p(\boldsymbol{f}|\boldsymbol{g}, \boldsymbol{q})\} = \arg\min_{\boldsymbol{f}} \{J(\boldsymbol{f})\}$$

$$J(\boldsymbol{f}) = \|\boldsymbol{g} - \boldsymbol{H}\boldsymbol{f}\|^2 + \sum_{\boldsymbol{r}} (1 - q(\boldsymbol{r})) \left(f(\boldsymbol{r}) - \beta \sum_{\boldsymbol{r}' \in \mathcal{V}(\boldsymbol{r})} f(\boldsymbol{r}') \right)^2$$

$$\widehat{\boldsymbol{q}} = \arg\max_{\boldsymbol{q}} \{p(\boldsymbol{q}|\boldsymbol{g})\}$$

$=$

$$\widehat{\boldsymbol{f}} = \arg\min_{\boldsymbol{f}} \{J_1(\boldsymbol{f}|\boldsymbol{g})\}$$

$$J_1(\boldsymbol{f}) = \|\boldsymbol{g} - \boldsymbol{H}\boldsymbol{f}\|^2 + \sum_{\boldsymbol{r}} \phi \left(f(\boldsymbol{r}) - \beta \sum_{\boldsymbol{r}' \in \mathcal{V}(\boldsymbol{r})} f(\boldsymbol{r}') \right)$$

$$\phi(t) = \begin{cases} |t|^2 & \text{if } |t| < \alpha, \\ \alpha^2 & \text{else,} \end{cases}$$

Modèles markoviens avec variables cachées étiquettes régions

$\boldsymbol{g} = \boldsymbol{H}\boldsymbol{f} + \boldsymbol{\epsilon}$

$\boldsymbol{f}$ représente l'image d'un objet composé d'un nombre finie de matériaux homogènes

Variables cachée étiquettes

$z(\boldsymbol{r}) = k, \quad k = 1, \cdots, K$

$\mathcal{R}_k = \{\boldsymbol{r} \;:\; z(\boldsymbol{r}) = k\}, \quad \mathcal{R} = \cup_k \mathcal{R}_k$

$p(f(\boldsymbol{r})|z(\boldsymbol{r}) = k) = \mathcal{N}(f(\boldsymbol{r})|m_k, \sigma_k^2)$

$\boldsymbol{z} = \{z(\boldsymbol{r}), \boldsymbol{r} \in \mathcal{R}\}$ image segmentée

Champ de Potts:

$$p(\boldsymbol{z}) \propto \exp\left[\alpha \sum_{\boldsymbol{r}\in\mathcal{R}} \sum_{\boldsymbol{r}'\in\mathcal{V}(\boldsymbol{r})} \delta(z(\boldsymbol{r}) - z(\boldsymbol{r}'))\right]$$

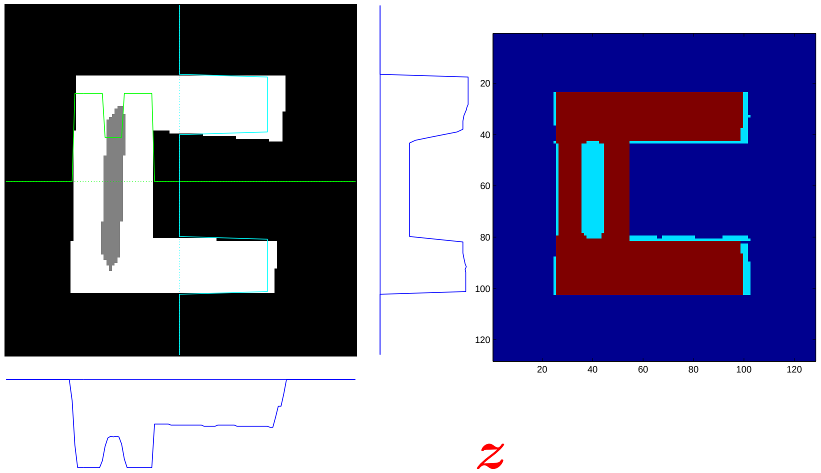

$\boldsymbol{z}$

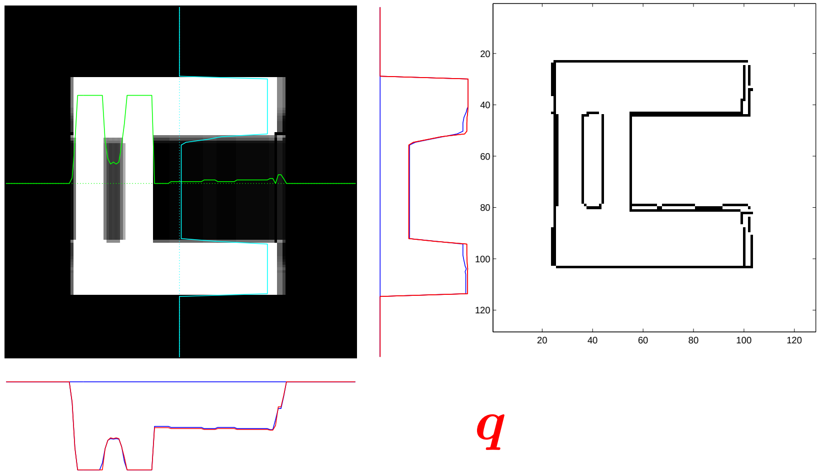

$\boldsymbol{q}$

- Mélange de gaussiennes avec $\{z(\boldsymbol{r}), \boldsymbol{r} \in \mathcal{R}\}$ i.i.d.

$$p(\boldsymbol{z}) = \prod_{k=1}^{K} p_k \qquad \text{avec} \qquad P(z(\boldsymbol{r}) = k) = p_k \quad \text{et} \quad \sum_{k=1}^{K} p_k = 1$$

- Mélange de gaussiennes avec un modèle de Potts pour $\boldsymbol{z}$

$$p(\boldsymbol{z}) \propto \exp\left[\alpha \sum_{\boldsymbol{r}\in\mathcal{R}} \sum_{\boldsymbol{r}'\in\mathcal{V}(\boldsymbol{r})} \delta(z(\boldsymbol{r}) - z(\boldsymbol{r}'))\right]$$

- Hyperparamètres $\boldsymbol{\theta} = \{{\sigma_\epsilon}^2, (m_k, \sigma_k^2), k = 1, \cdots, K\}$:

$$p(m_k) = \mathcal{N}(m_k | m_{k_0}, \sigma_{k_0}^2), \qquad p(\sigma_k^2) = \mathcal{IG}(\sigma_k^2 | \alpha_{k0}, \beta_{k0}),$$
$$p(\boldsymbol{\Sigma}_k) = \mathcal{IW}(\boldsymbol{\Sigma}_k | \alpha_{k0}, \boldsymbol{\Lambda}_{k0}), \quad p({\sigma_{\epsilon}}_i^2) = \mathcal{IG}({\sigma_{\epsilon}}_i^2 | \alpha_0^{\epsilon_i}, \beta_0^{\epsilon_i}).$$

- Loi *a posteriori* conjointe de $\boldsymbol{f}$, $\boldsymbol{z}$ et $\boldsymbol{\theta}$

$$p(\boldsymbol{f}, \boldsymbol{z}, \boldsymbol{\theta} | \boldsymbol{g}) \propto p(\boldsymbol{g} | \boldsymbol{f}, \boldsymbol{\theta}_1)\, p(\boldsymbol{f} | \boldsymbol{z}, \boldsymbol{\theta}_2)\, p(\boldsymbol{z} | \boldsymbol{\theta}_3)\, p(\boldsymbol{\theta})$$

Estimation de $\boldsymbol{f}$ lorsque $\boldsymbol{\theta}$ et $\boldsymbol{z}$ sont connus:

MAP: $\widehat{\boldsymbol{f}} = \arg\max_{\boldsymbol{f}} \{p(\boldsymbol{f}|\boldsymbol{g},\boldsymbol{z},\boldsymbol{\theta})\} = \arg\min_{\boldsymbol{f}} \{\boldsymbol{J}(\boldsymbol{f}|\boldsymbol{g},\boldsymbol{z},\boldsymbol{\theta})\}$.

- avec un modèle i.i.d. :

$$J(\boldsymbol{f}|\boldsymbol{g},\boldsymbol{z},\boldsymbol{\theta}) = ||\boldsymbol{g}-\boldsymbol{H}\boldsymbol{f}||^2 + \lambda \sum_{k=1}^{K} \sum_{\boldsymbol{r}\in\mathcal{R}_k} \frac{||f(\boldsymbol{r})-m_k||^2}{\sigma_k^2}$$

- avec modèle markovien : $\widetilde{\boldsymbol{f}}_k = \boldsymbol{f}_k - m_k\mathbf{1}$

$$J(\boldsymbol{f}|\boldsymbol{g},\boldsymbol{z},\boldsymbol{\theta}) = ||\boldsymbol{g}-\boldsymbol{H}\boldsymbol{f}||^2 + \lambda \sum_{k=1}^{K} \sum_{\boldsymbol{r}\in\mathcal{R}_k} \frac{1}{\sigma_k^2}\left(\widetilde{f}(\boldsymbol{r}) - \beta_{\boldsymbol{r}} \sum_{\boldsymbol{r}'\in(\mathcal{V}(\boldsymbol{r})\cap\mathcal{R}_k)} \widetilde{f}(\boldsymbol{r}')\right)^2$$

$$= ||\boldsymbol{g}-\boldsymbol{H}\boldsymbol{f}||^2 + \lambda \sum_{\boldsymbol{r}\in\mathcal{R}} (1-q(\boldsymbol{r}))\left(f(\boldsymbol{r}) - \sum_{\boldsymbol{r}'\in\mathcal{V}(\boldsymbol{r})} (1-q(\boldsymbol{r}'))f(\boldsymbol{r}')\right)^2$$

$$+\lambda \sum_{k=1}^{K} \sum_{\boldsymbol{r}\in\mathcal{R}_k} \left(\frac{f(\boldsymbol{r})-m_k}{\sigma_k}\right)^2$$

où $\widetilde{f}(\boldsymbol{r}) = f(\boldsymbol{r}) - m(\boldsymbol{r})$, $\beta_{\boldsymbol{r}} = \frac{1}{n_{\boldsymbol{r}}}$, $n_{\boldsymbol{r}} = Card(\mathcal{V}(\boldsymbol{r}) \cap \mathcal{R}_k)$.

Estimation conjointe de $(\boldsymbol{f}, \boldsymbol{z}, \boldsymbol{\theta})$ utilisant $p(\boldsymbol{f}, \boldsymbol{z}, \boldsymbol{\theta}|\boldsymbol{g})$

$$\left\{\begin{array}{lll}
\widehat{\boldsymbol{\theta}} & \sim & p(\boldsymbol{\theta}|\widehat{\boldsymbol{f}}, \widehat{\boldsymbol{z}}, \boldsymbol{g}) \quad \text{ou} \quad p(\boldsymbol{\theta}|\widehat{\boldsymbol{z}}, \boldsymbol{g}) \\
\widehat{\boldsymbol{z}} & \sim & p(\boldsymbol{z}|\widehat{\boldsymbol{f}}, \widehat{\boldsymbol{\theta}}, \boldsymbol{g}) \quad \text{ou} \quad p(\boldsymbol{z}|\widehat{\boldsymbol{\theta}}, \boldsymbol{g}) \\
\widehat{\boldsymbol{f}} & \sim & p(\boldsymbol{f}|\widehat{\boldsymbol{z}}, \widehat{\boldsymbol{\theta}}, \boldsymbol{g})
\end{array}\right.$$

où $\sim$ signifie soit $\arg\max$ soit échantllonner suivant

$$\left\{\begin{array}{rcll}
p(\boldsymbol{f}|\boldsymbol{z}, \boldsymbol{\theta}, \boldsymbol{g}) & = & p(\boldsymbol{g}|\boldsymbol{f}, \boldsymbol{\theta}_1)\, p(\boldsymbol{f}|\boldsymbol{z}, \boldsymbol{\theta}_2)/p(\boldsymbol{g}|\boldsymbol{z}, \boldsymbol{\theta}) & \text{Gaussienne} \\
p(\boldsymbol{z}|\boldsymbol{f}, \boldsymbol{\theta}, \boldsymbol{g}) & \propto & p(\boldsymbol{g}|\boldsymbol{f}, \boldsymbol{\theta}_1)\, p(\boldsymbol{f}|\boldsymbol{z}, \boldsymbol{\theta}_2)\, p(\boldsymbol{z}) & \text{Potts} \\
p(\boldsymbol{z}|\boldsymbol{\theta}, \boldsymbol{g}) & = & p(\boldsymbol{g}|\boldsymbol{z}, \boldsymbol{\theta})\, p(\boldsymbol{z})/p(\boldsymbol{g}|\boldsymbol{\theta}) & \text{Potts} \\
p(\boldsymbol{\theta}|\boldsymbol{f}, \boldsymbol{z}, \boldsymbol{g}) & = & p(\boldsymbol{g}|\boldsymbol{f}, \boldsymbol{\theta}_1)\, p(\boldsymbol{f}|\boldsymbol{z}, \boldsymbol{\theta}_2)\, p(\boldsymbol{\theta})/p(\boldsymbol{g}) & \text{Gaussienne/Inverse Gamma} \\
p(\boldsymbol{\theta}|\boldsymbol{z}, \boldsymbol{g}) & = & p(\boldsymbol{g}|\boldsymbol{z}, \boldsymbol{\theta})\, p(\boldsymbol{\theta})/p(\boldsymbol{g}) & \text{Gaussienne/Inverse Gamma}
\end{array}\right.$$

$\boldsymbol{\theta}_1 = {\sigma_\epsilon}^2$, $\boldsymbol{\theta}_2 = \{(m_k, \sigma_k^2), k = 1, \cdots, K\}$, $\boldsymbol{\theta} = (\boldsymbol{\theta}_1, \boldsymbol{\theta}_2)$

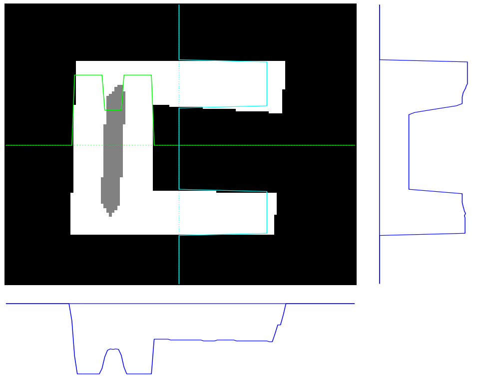

Original

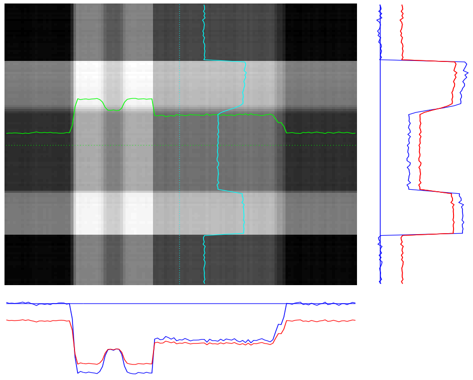

Backprojection

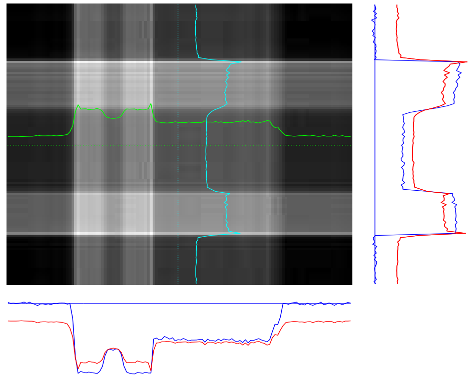

Filtered BP

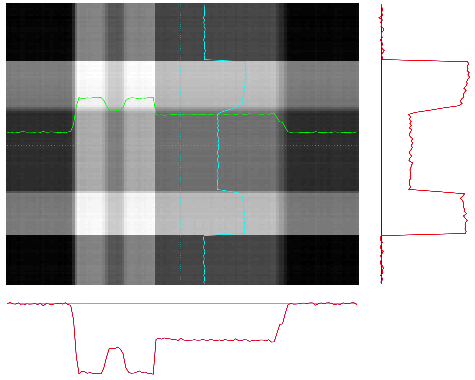

LS

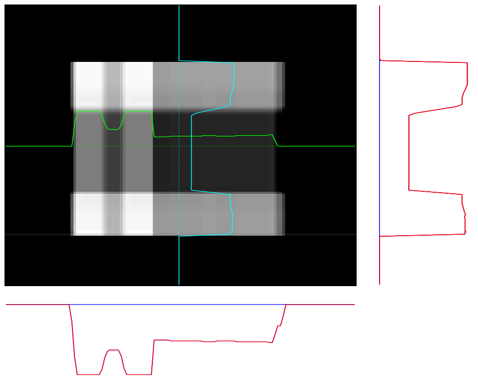

Gauss-Markov+pos+supp $\boldsymbol{f}$

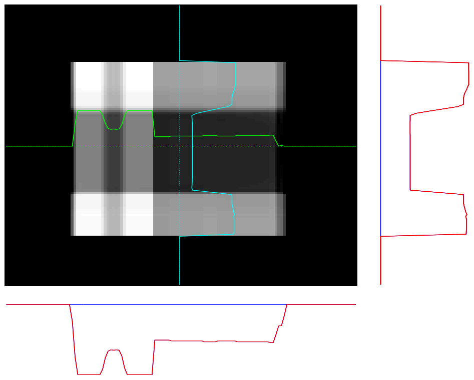

GM+Line process $\boldsymbol{f}$, $\boldsymbol{q}$

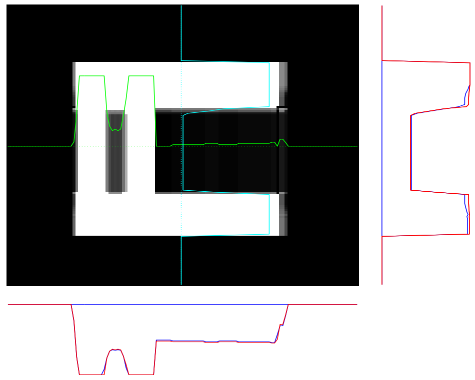

GM+Label process $\boldsymbol{f}$, $\boldsymbol{z}$

$\boldsymbol{q}$

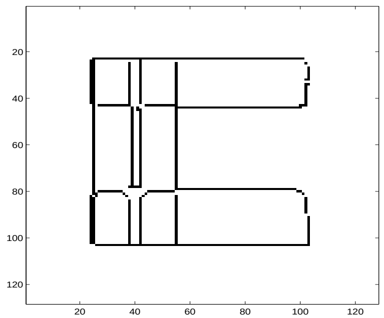

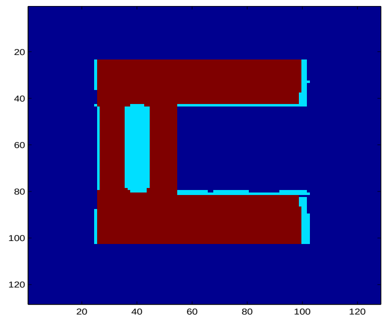

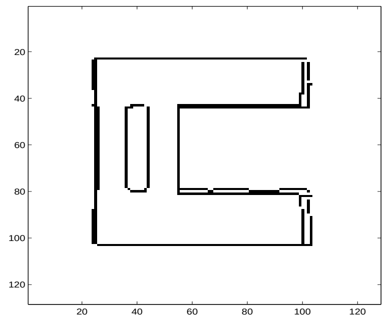

Fusion d'image et segmentation jointe

(Olivier FÉRON)

$$\left\{\begin{array}{l} g_i(\boldsymbol{r}) = f_i(\boldsymbol{r}) + \epsilon_i(\boldsymbol{r}) \\ p(f_i(\boldsymbol{r})|z(\boldsymbol{r}) = k) = \mathcal{N}(m_{ik}, \sigma_{ik}) \\ p(\underline{\boldsymbol{f}}|\boldsymbol{z}) = \prod_i p(\boldsymbol{f}_i|\boldsymbol{z}) \end{array}\right.$$

$\boldsymbol{g}_1$

$\boldsymbol{g}_2$

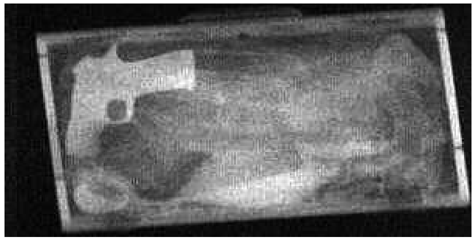

$\longrightarrow$

$\widehat{\boldsymbol{f}}_1$

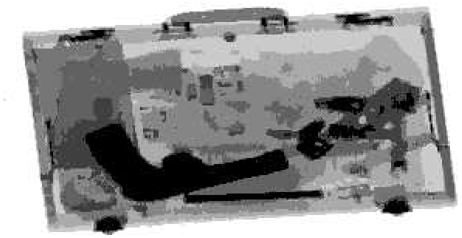

$\widehat{\boldsymbol{f}}_2$

$\widehat{\boldsymbol{z}}$

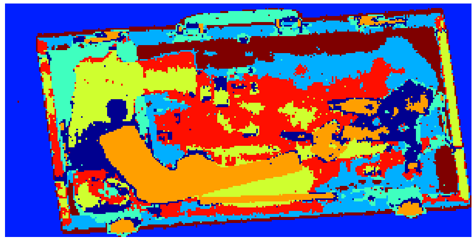

Fusion d'image en imagerie médicale

(Olivier FÉRON)

g_1 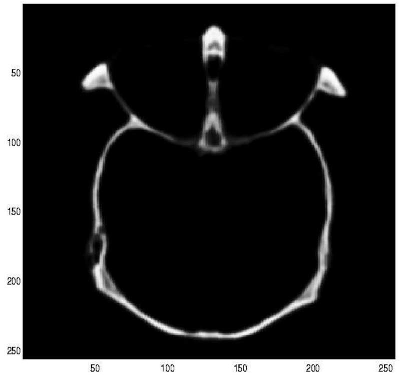

$\longrightarrow$

$\widehat{f}_1$ 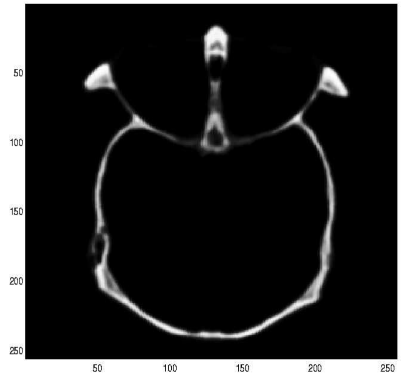

$\widehat{z}$ 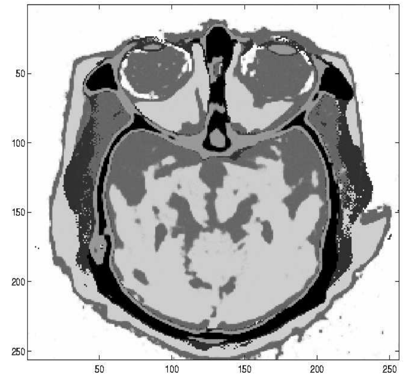

g_2 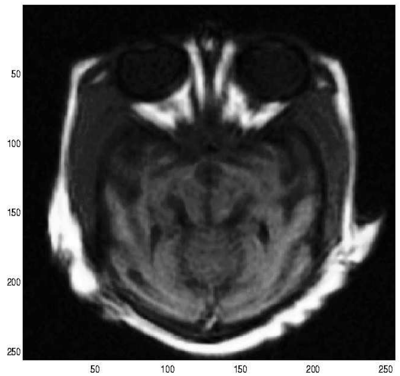

$\widehat{f}_2$ 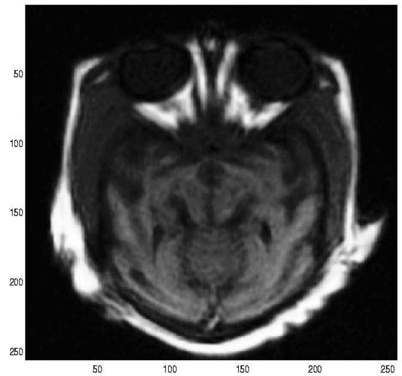

Ségmentation conjoint des images hyper-spectrales

(Adel MOHAMMADPOUR)

$$\begin{cases} g_i(\boldsymbol{r}) = f_i(\boldsymbol{r}) + \epsilon_i(\boldsymbol{r}) \\ p(f_i(\boldsymbol{r})|z(\boldsymbol{r}) = k) = \mathcal{N}(m_{i\,k}, \sigma_{i\,k}), \quad k = 1, \cdots, K \\ p(\underline{\boldsymbol{f}}|\boldsymbol{z}) = \prod_i p(\boldsymbol{f}_i|\boldsymbol{z}) \\ m_{i\,k} \;\; \text{markovienne le long de l'index} \;\; i \end{cases}$$

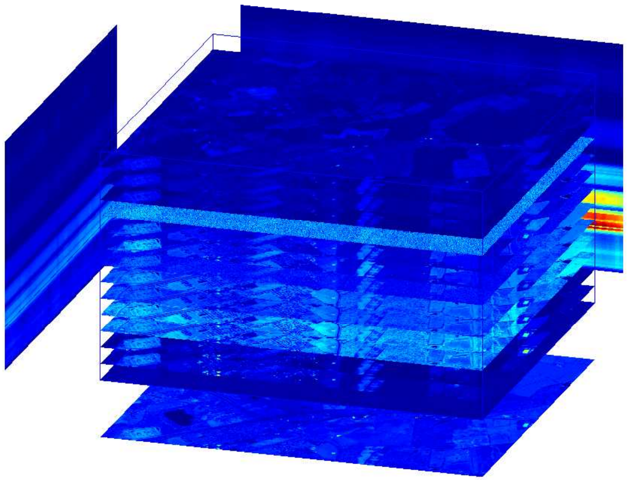

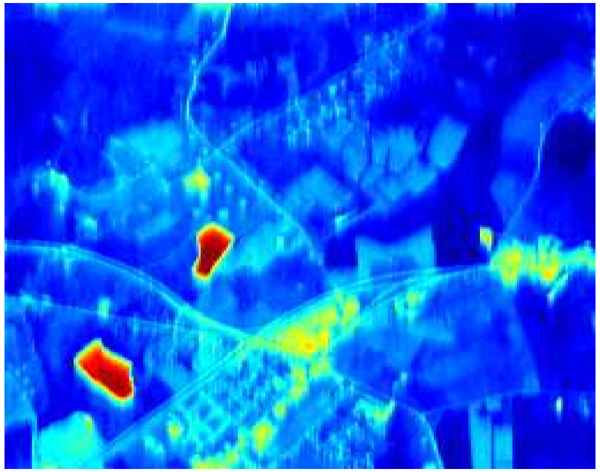

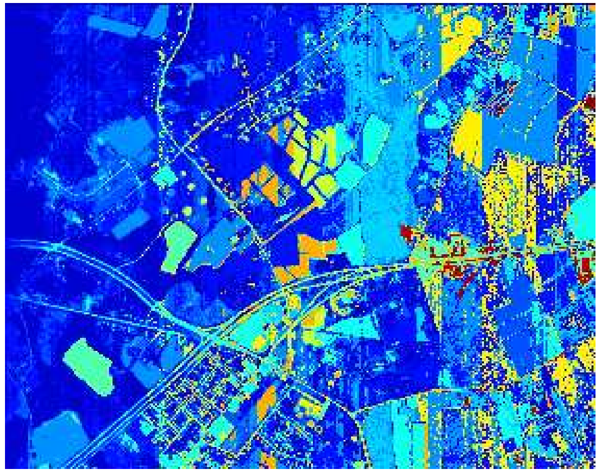

Ségmentation d'une séquence vidéo

(Patrice BRAULT)

$$\begin{cases} g_i(\boldsymbol{r}) = f_i(\boldsymbol{r}) + \epsilon_i(\boldsymbol{r}) \\ p(f_i(\boldsymbol{r})|z_i(\boldsymbol{r}) = k) = \mathcal{N}(m_{ik}, \sigma_{ik}), \quad k = 1, \cdots, K \\ p(\underline{\boldsymbol{f}}|\boldsymbol{z}) = \prod_i p(\boldsymbol{f}_i|\boldsymbol{z}_i) \\ z_i(\boldsymbol{r}) \text{ markovien le long de l'index } i \end{cases}$$

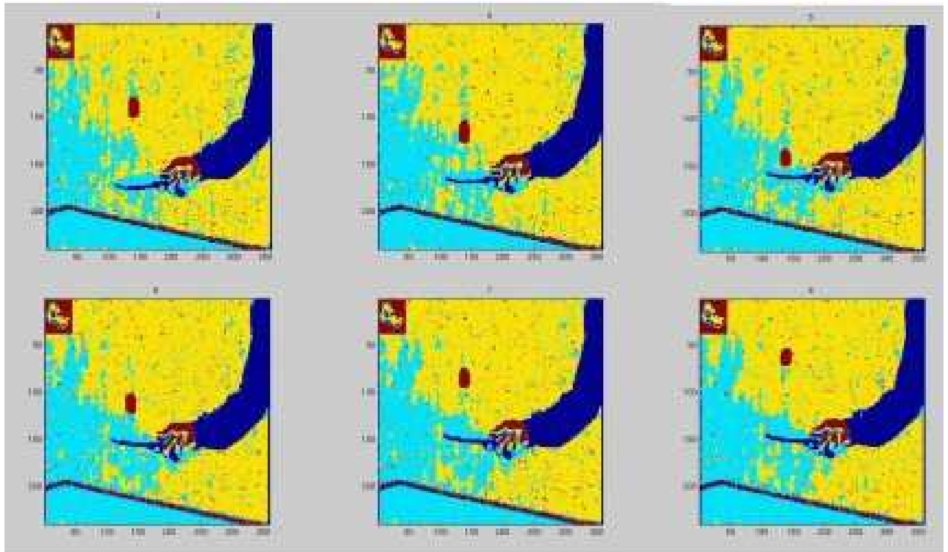

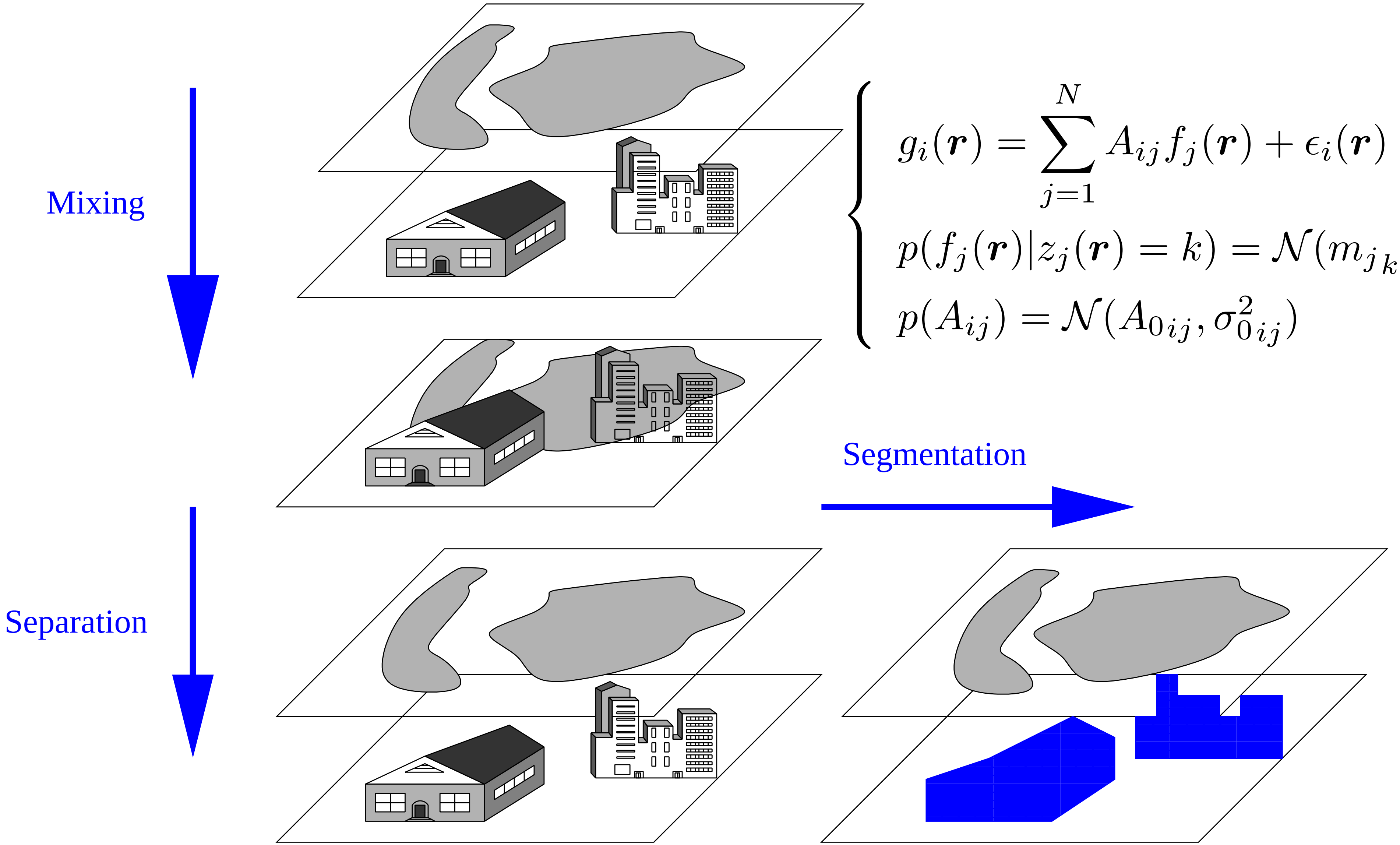

$$
\left\{
\begin{array}{l}
g_i(\boldsymbol{r}) = \sum_{j=1}^{N} A_{ij} f_j(\boldsymbol{r}) + \epsilon_i(\boldsymbol{r}) \\
p(f_j(\boldsymbol{r}) | z_j(\boldsymbol{r}) = k) = \mathcal{N}(m_{j\,k}, \sigma^2_{j\,k}) \\
p(A_{ij}) = \mathcal{N}(A_{0\,ij}, \sigma^2_{0\,ij})
\end{array}
\right.
$$

Séparation et ségmentation des images

(H. Snoussi)

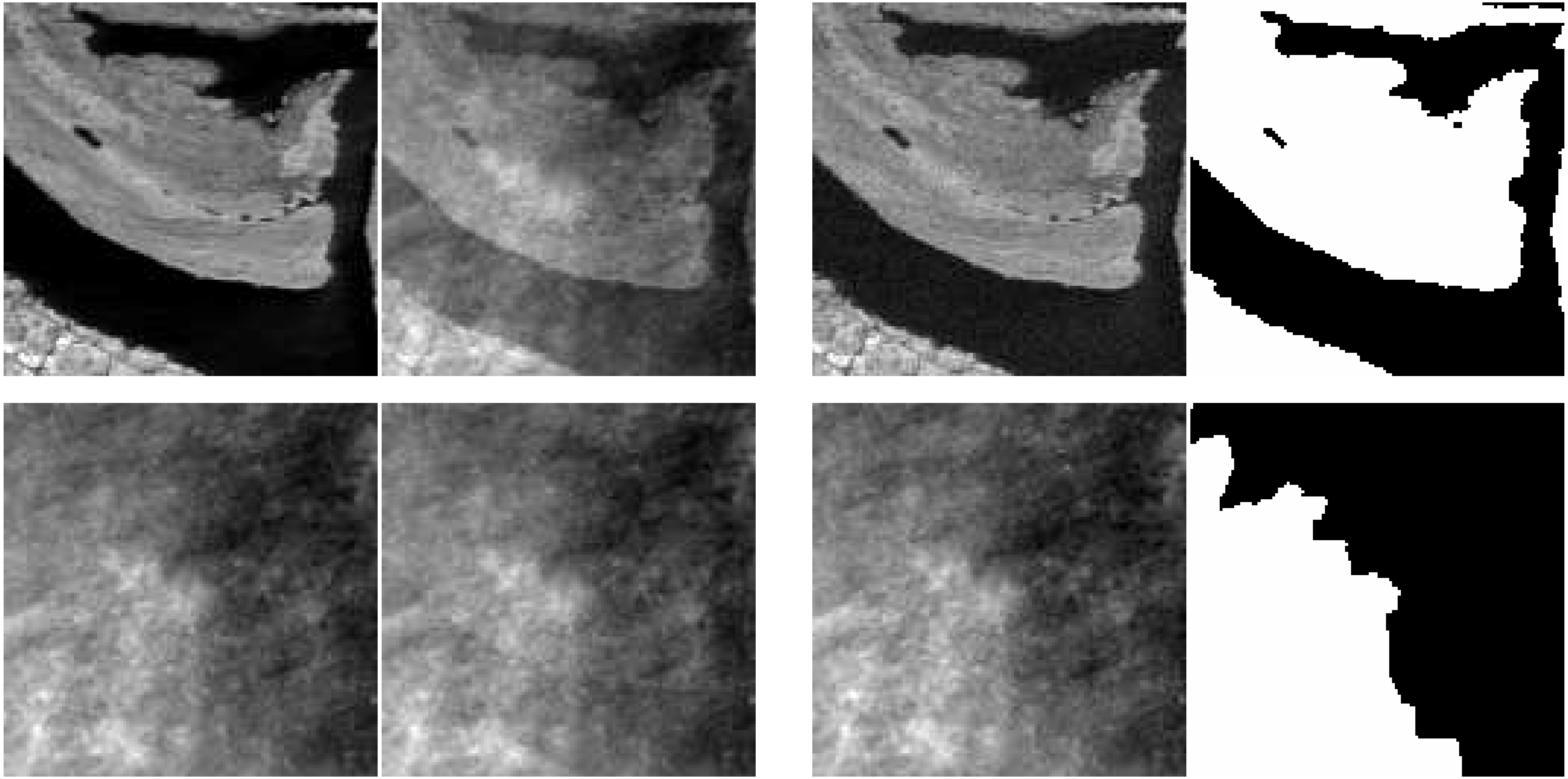

$\underline{\boldsymbol{f}}$ $\underline{\boldsymbol{g}}$ $\underline{\widehat{\boldsymbol{f}}}$ $\underline{\widehat{\boldsymbol{z}}}$

Synthèse de Fourier en imagerie microondes

(O. Féron en collaboration avec DRÉ)

$$g(\boldsymbol{\omega}) = \int f(\boldsymbol{r}) \exp\left[-j(\boldsymbol{\omega}.\boldsymbol{r})\right] \,\mathrm{d}\boldsymbol{r} + \epsilon(\boldsymbol{\omega})$$

$$g(u,v) = \int f(x,y) \exp\left[-j(ux+vy)\right] \,\mathrm{d}x\,\mathrm{d}y + \epsilon(u,v)$$

$$\boldsymbol{g} = \boldsymbol{H}\boldsymbol{f} + \boldsymbol{\epsilon}$$

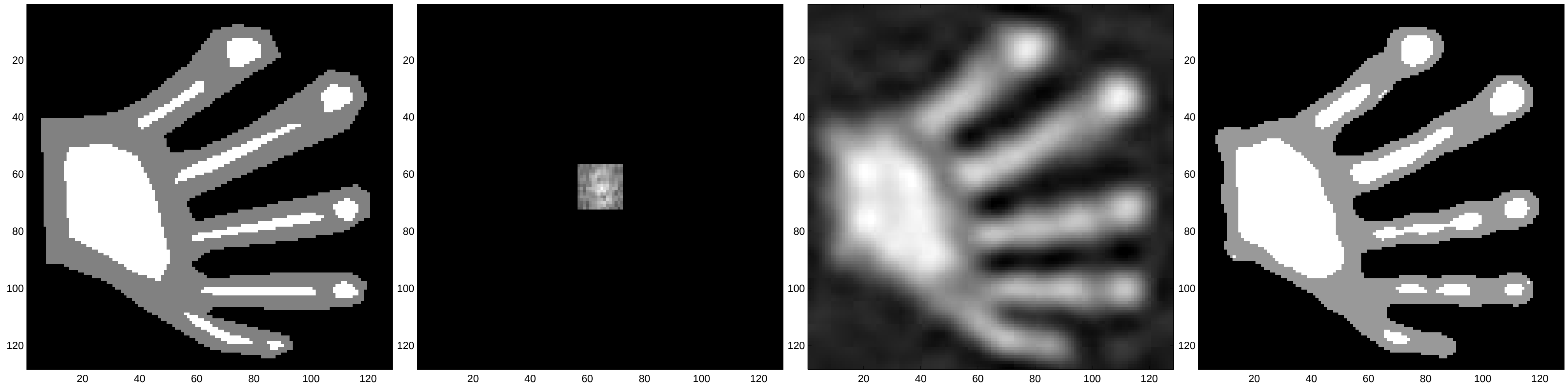

$f(x,y)$ $\quad$ $g(u,v)$ $\quad$ $\widehat{\boldsymbol{f}}$ par FFTI $\quad$ $\widehat{\boldsymbol{f}}$ méthode proposée

Séparation d'images dans le domaine des ondelettes

$$\boldsymbol{g}(\boldsymbol{r}) = \boldsymbol{f}(\boldsymbol{r}) + \boldsymbol{\epsilon}(\boldsymbol{r}) \longrightarrow \mathrm{WT} \longrightarrow \widetilde{\boldsymbol{g}}^j(\boldsymbol{r}) = \widetilde{\boldsymbol{f}}^j(\boldsymbol{r}) + \widetilde{\boldsymbol{\epsilon}}^j(\boldsymbol{r})$$

images | Hist. des images | Coéff. ondelettes | Hist. des coéff.

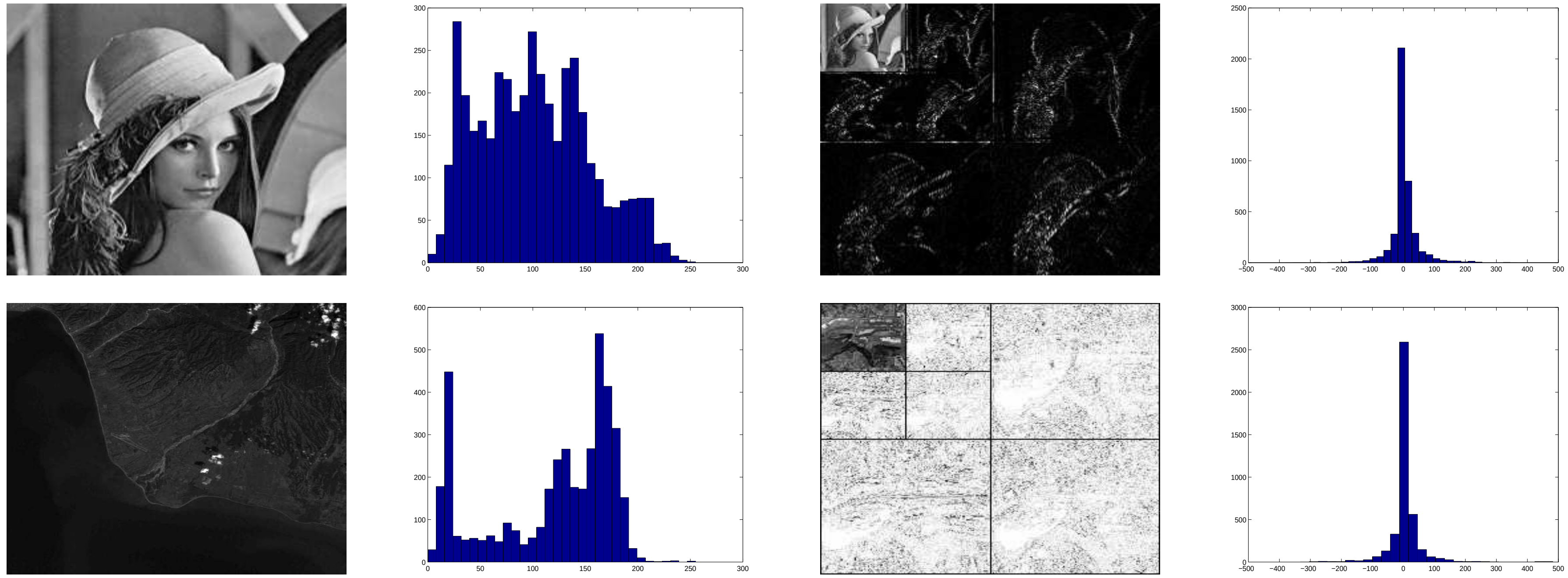

- multi-résolution
- Coéfficients d'ondelettes peuvent souvent être classés en $K=2$ classes

Séparation d'images dans le domaine des ondelettes

(M. Ichir)

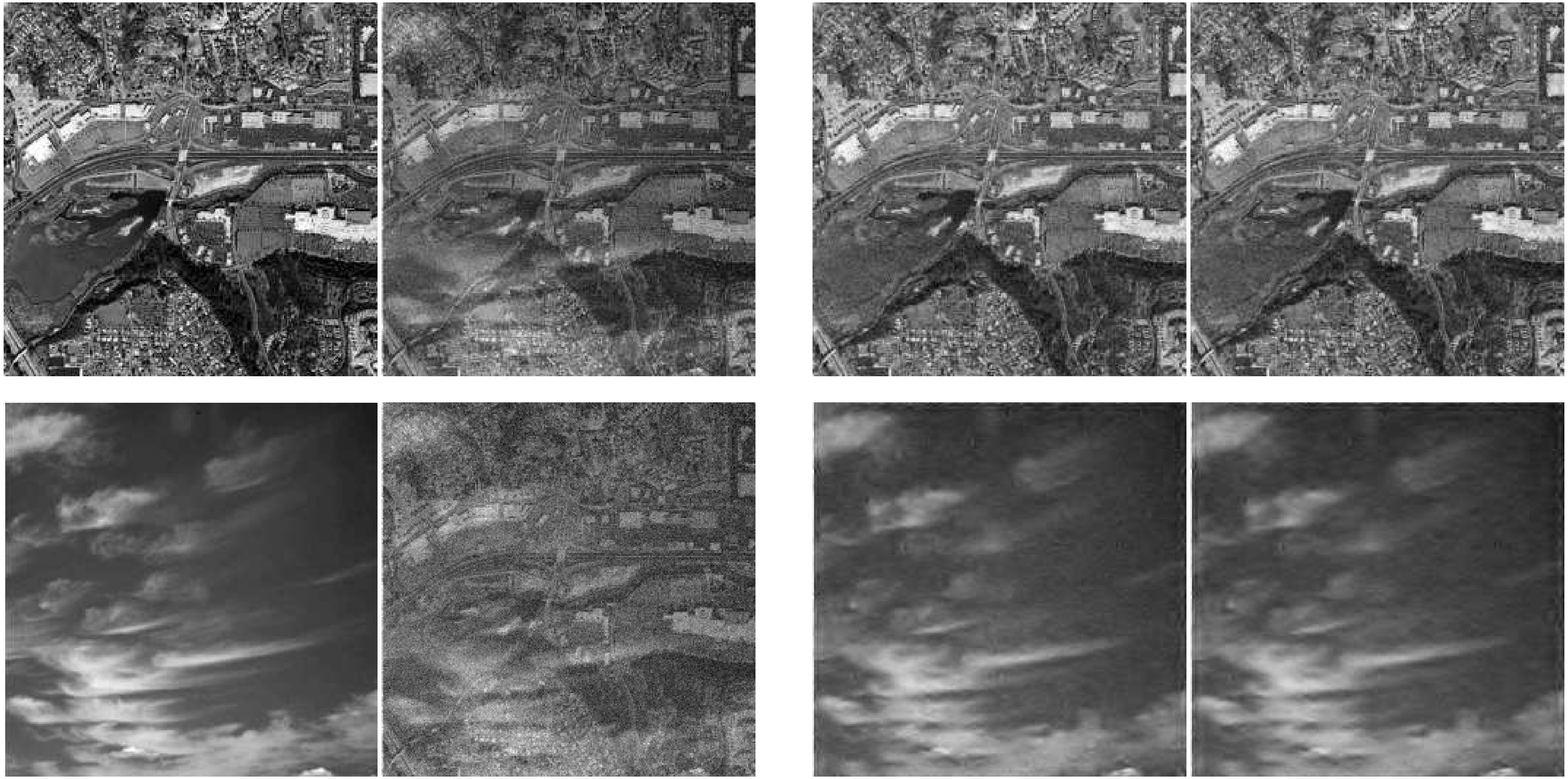

$\underline{\boldsymbol{f}}$ $\underline{\boldsymbol{g}}$ $\underline{\widehat{\boldsymbol{f}}}$ (GM) $\underline{\widehat{\boldsymbol{f}}}$ (HMM)

Super-résolution

(F. Humblot)

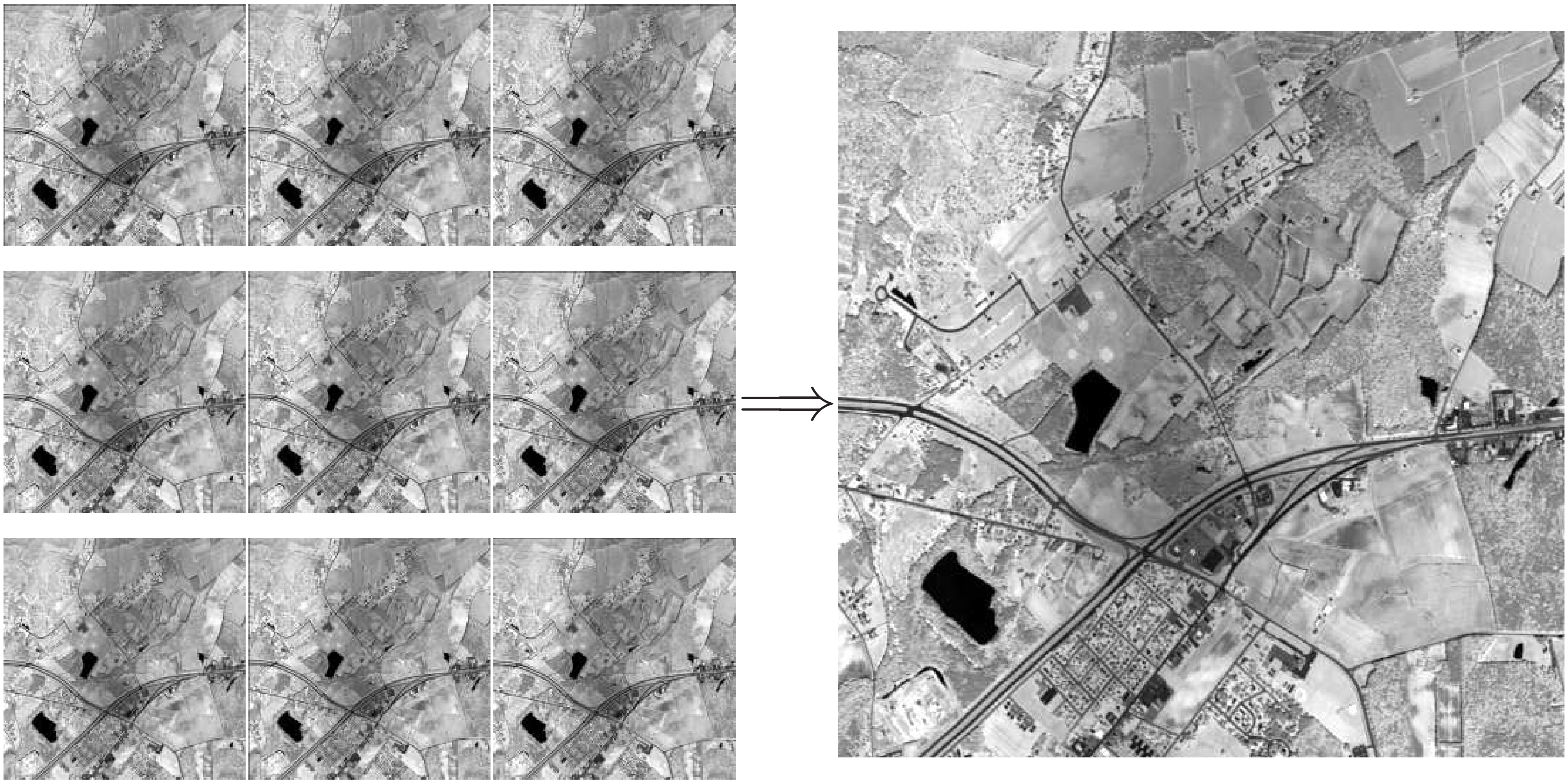

Séparation de sources

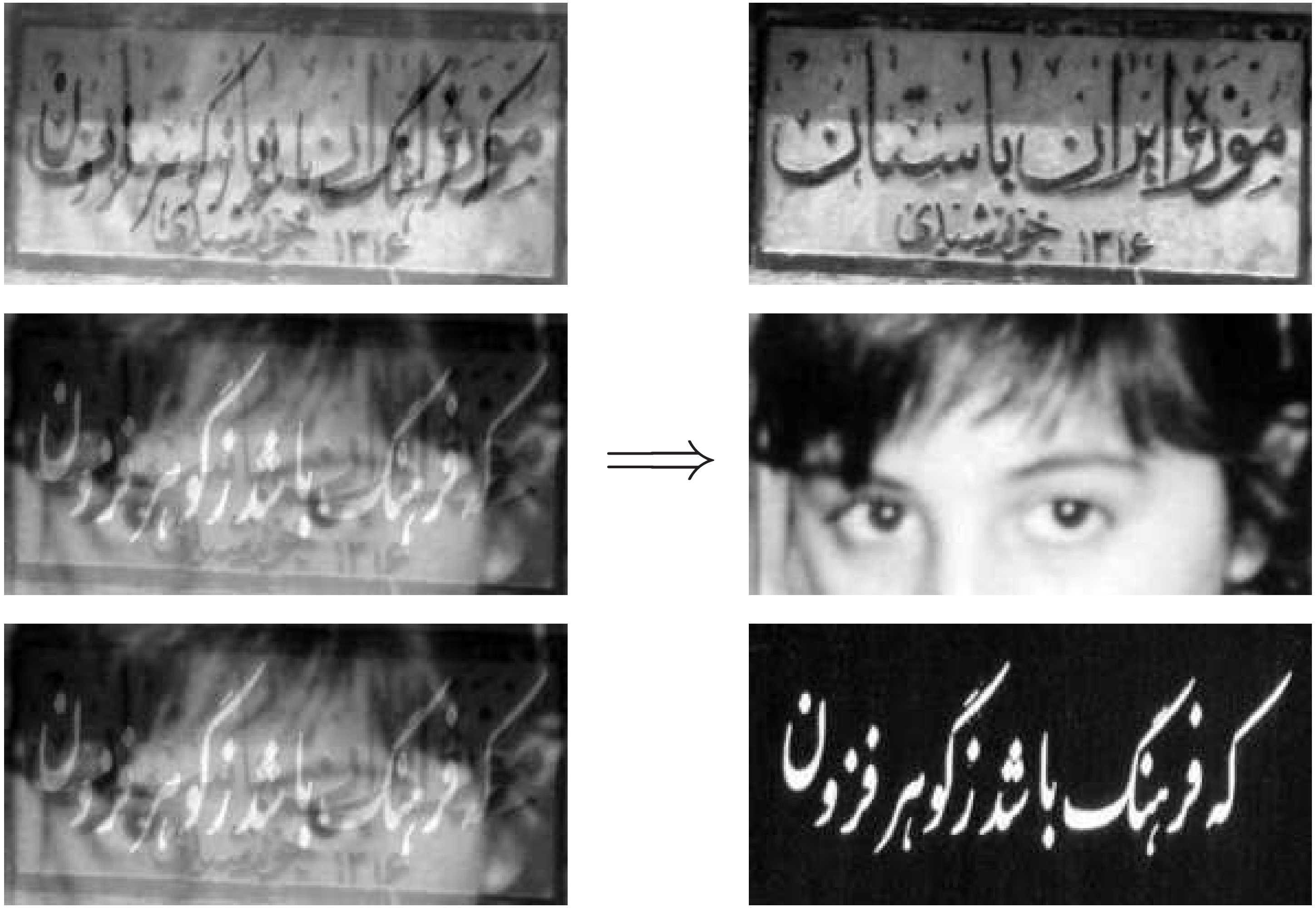

Ségmentation et réduction de données en imagerie hyper-spectrale

(N. Bali)

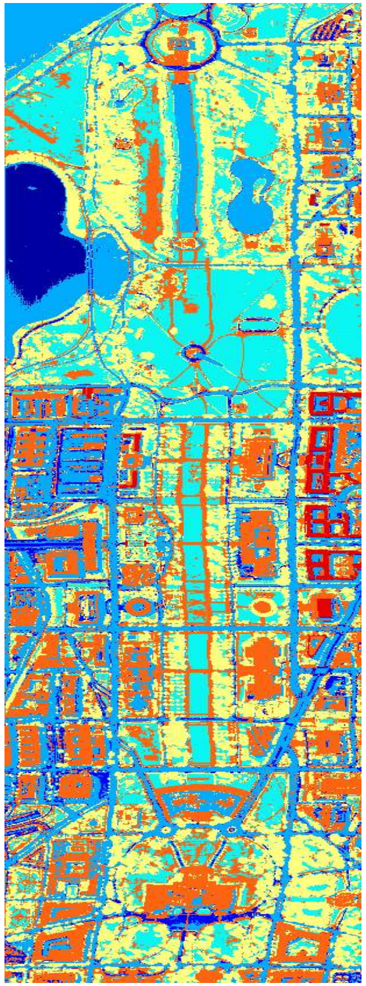

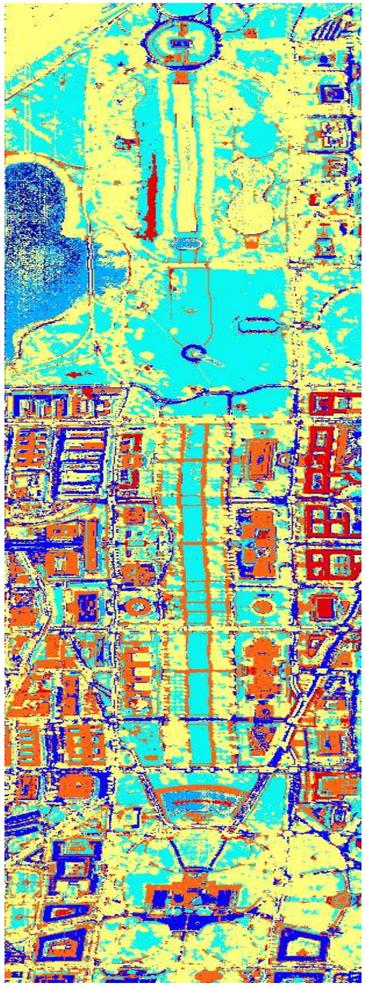

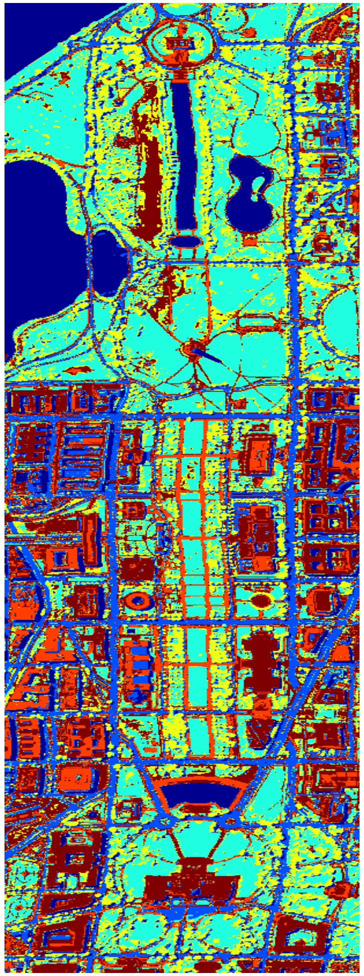

Originale Classique (47%) Méthode proposée (82%)

Tomographie 3D pour CND

(en collaboration avec EDF)

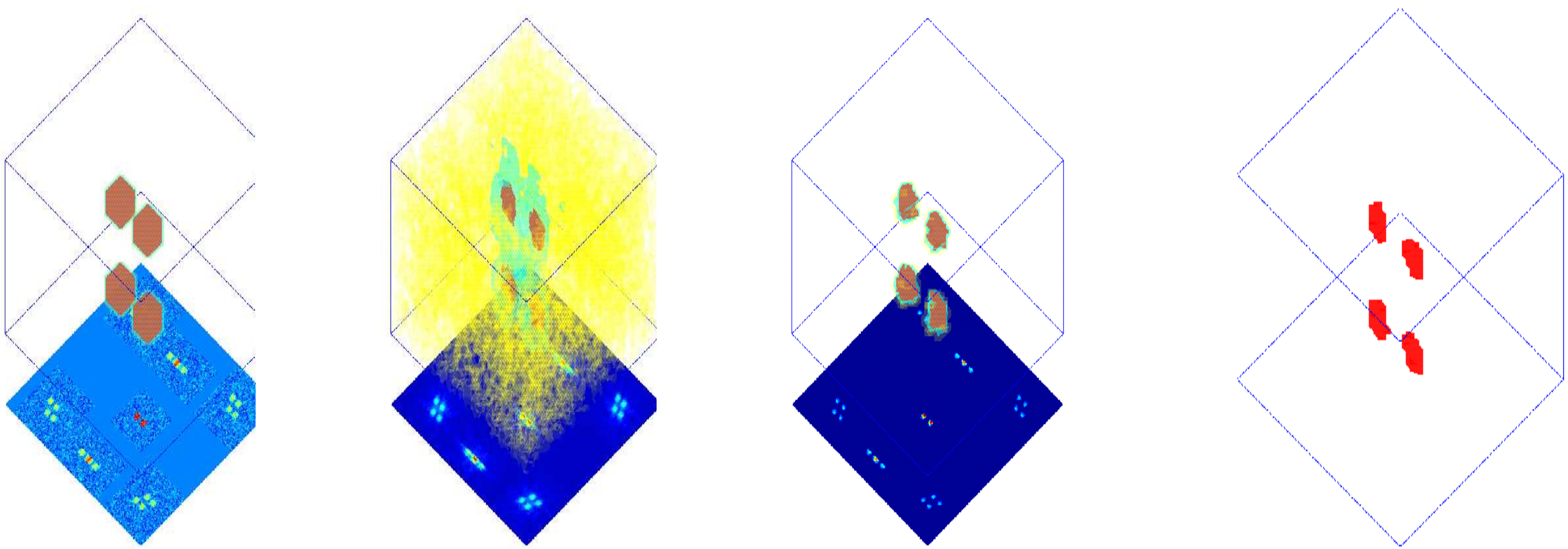

Originale | Rétroprojection | Méthode proposée $\boldsymbol{f}$ | Méthode proposée $\boldsymbol{z}$

Conclusions

Approche bayésienne et les modèles markoviens avec des variables cachées sont des outils d'inférence bien appropriés pour grand nombre de problèmes inverses en traitement du signal et d'image

- H. Snoussi: Séparation de sources 1D et 2D
- M. Ichir: Séparation de sources dans le domaine des ondelettes
- S. Moussaoui: Séparation de sources positives et application en spéctrométrie
- O. Féron : Fusion d'image et problèmes inverses en imageries microondes
- P. Brault: Segmentation de séquance d'images
- A. Mohammadpour: Classification et segmentation d'images hyper-spectrales,
- F. Humblot: Super-résolution
- N. Bali : Séparation de sources pour la classification et réduction de données en imagerie hyper-spectrale
- S. Fekih-Salem: Tomographie 3D des micro structures (collaboration avec CEA)
- L. Robillard: Tomographie 3D en contrôle non destructif (CND) (collaboration avec EDF)

References

[1] M. M. Ichir and A. Mohammad-Djafari, "Hidden markov models for blind source separation," *IEEE Trans. on Signal Processing*, vol. 15, pp. 1887–1899, Jul 2006.

[2] S. Moussaoui, D. Brie, A. Mohammad-Djafari, and C. Carteret, "Separation of non-negative mixture of non-negative sources using a bayesian approach and mcmc sampling," *IEEE Trans. on Signal Processing*, vol. 54, p. 1:14, Nov 2006.

[3] A. Mohammad-Djafari and L. Robillard, "Hierarchical markovian models for 3d computed tomography in non destructive testing applications," in *EUSIPCO 2006*, EUSIPCO 2006, September 4-8, Florence, Italy, September 2006.

[4] N. Bali and A. Mohammad-Djafari, "Joint dimensionality reduction, classification and segmentation of hyperspectral images," in *ICIP 2006*, ICIP06, October 8-11, Atlanta, GA, USA., October 2006.

[5] F. Humblot and A. Mohammad-Djafari, "Super-Resolution using Hidden Markov Model and Bayesian Detection Estimation Framework," *EURASIP Journal on Applied Signal Processing*, vol. Special number on Super-Resolution Imaging: Analysis, Algorithms, and Applications, pp. ID 36971, 16 pages, 2006.

[6] O. Féron, D. B., and A. Mohammad-Djafari, "Microwave imaging of inhomogeneous objects made of a finite number of dielectric and conductive materials from experimental data," *Inverse Problems*, vol. 21, pp. 95–115, Dec 2005.

[7] P. Brault and A. Mohammad-Djafari, "Unsupervised bayesian wavelet domain segmentation using a potts-markov random field modeling," *Journal of Electronic Imaging*, vol. 14, pp. 043011–1:043011–16, Oct-Dec 2005.

[8] O. Féron and A. Mohammad-Djafari, "Image fusion and joint segmentation using an MCMC algorithm," *Journal of Electronic Imaging*, vol. 14, p. paper no. 023014, Apr 2005.

[9] H. Snoussi and A. Mohammad-Djafari, "Bayesian unsupervised learning for source separation with mixture of gaussians prior," *Journal of VLSI Signal Processing Systems*, vol. 37, pp. 263–279, June/July 2004.

[10] H. Snoussi and A. Mohammad-Djafari, "Fast joint separation and segmentation of mixed images," *Journal of Electronic Imaging*, vol. 13, pp. 349–361, April 2004.

[11] H. Snoussi and A. Mohammad-Djafari, "Estimation of structured gaussian mixtures: the inverse em algorithm," *IEEE Trans. on Signal Processing*, vol. accepted, no. to appear, 2006.

[12] C. Soussen and A. Mohammad-Djafari, "Polygonal and polyhedral contour reconstruction in computed tomography," *IEEE Trans. on Image Processing*, vol. 13, pp. 1507–1523, Nov 2004.

[13] A. Mohammad-Djafari, J.-F. Giovannelli, G. Demoment, and J. Idier, "Regularization, maximum entropy and probabilistic methods in mass spectrometry data processing problems," *Int. Journal of Mass Spectrometry*, vol. 215, pp. 175–193, April 2002.

[14] O. Féron, *Approche bayésienne en séparation de sources. Applications en imagerie.* Phd thesis, Université de Paris–Sud, Orsay, France, September 2006.

[15] P. Brault, *Approche bayésienne en séparation de sources. Applications en imagerie.* Phd thesis, Université de Paris–Sud, Orsay, France, September 2005.

[16] F. Humblot, *Dtection de petits objets dans une image en utilisant les techniques de super-rsolution.* Phd thesis, Université de Paris–Sud, Orsay, France, September 2005.

[17] M. M. Ichir, *Estimation bayésienne et approche multi-rsolution en séparation de sources. Applications en imagerie.* Phd thesis, Université de Paris–Sud, Orsay, France, September 2005.

[18] H. Snoussi, *Approche bayésienne en séparation de sources. Applications en imagerie.* Phd thesis, Université de Paris–Sud, Orsay, France, September 2003.

[19] C. Soussen, *Reconstruction 3D d'un objet compact en tomographie*. Phd thesis, Université de Paris–Sud, Orsay, France, December 2000.

References

[1] S. Geman and D. Geman, "Stochastic relaxation, Gibbs distributions, and the Bayesian restoration of images," *IEEE Transactions on Pattern Analysis and Machine Intelligence*, vol. PAMI-6, pp. 721–741, Nov. 1984.

[2] D. Geman, "Random fields and inverse problems in imaging," in *Lecture Notes in Mathematics* (P. L. Hennequin, ed.), vol. 1427, pp. 117–193, Springer-Verlag, 1990.

[3] S. Geman and G. Reynolds, "Constrained restoration and recovery of discontinuities," *IEEE Transactions on Pattern Analysis and Machine Intelligence*, vol. PAMI-14, pp. 367–383, Mar 1992.

[4] J. E. Besag, "Spatial interaction and the statistical analysis of lattice systems," *Journal of the Royal Statistical Society B*, vol. 36, no. 2, pp. 192–236, 1974.

[5] J. E. Besag, "On the statistical analysis of dirty pictures," *Journal of the Royal Statistical Society B*, vol. 48, no. 3, pp. 259–302, 1986.

[6] J. Besag, "Digital image processing : Towards Bayesian image analysis," *Journal of Applied Statistics*, vol. 16, no. 3, pp. 395–407, 1989.

[7] J. Besag and P. Green, "Spatial statistics and Bayesian computation," *J. R. Statist. Soc. B*, vol. 55, pp. 25–37, 1993.

[8] A. Blake and A. Zisserman, *Visual reconstruction*. Cambridge: The MIT Press, 1987.

[9] M. Nikolova and A. Mohammad-Djafari, "Eddy current tomography using a binary Markov model," *To appear in Signal Processing*, vol. 49, pp. 000–000, May 1996.

[10] J. Idier, A. Mohammad-Djafari and G. Demoment "Regularization Methods and Inverse Problems: An Information Theory Standpoint," *Submitted to 2nd Intern. Conf. on Inverse Problems in Eng.*, Le Croisic, June 1996.